Schweizerische Eidgenossenschaft
Confédération suisse
Confederazione Svizzera
Confederaziun svizra

Eidgenössisches Departement für
Umwelt, Verkehr, Energie und Kommunikation UVEK

Bundesamt für Energie BFE
Energieforschung und Cleantech

Schlussbericht vom 30. April 2020

INFLOSCOM

Investigations into **IN**-nozzle **FLO**w, **S**pray and **COM**bustion

---

Datum: 30.04.2020

Ort: Bern

Subventionsgeberin:
Bundesamt für Energie BFE
Sektion Energieforschung und Cleantech
CH-3003 Bern
www.bfe.admin.ch

Ko-Finanzierung:
Combustion & Engine Research Center (CERC)
Chalmers University of Technology, 412 58 Göteborg, Sweden
www.chalmers.se\en\centres\cerc

Subventionsempfänger/innen:
Winterthur Gas & Diesel Ltd.
Schützenstrasse 1-3, 8400 Winterthur
www.wingd.com

Autor/in:
Reto Balz, Winterthur Gas & Diesel Ltd., reto.balz@wingd.com
Imre G. Nagy, Winterthur Gas & Diesel Ltd., imregergely.nagy@wingd.com

BFE-Projektbegleitung:
Carina Alles, carina.alles@bfe.admin.ch
Stephan Renz, info@renzconsulting.ch

BFE-Vertragsnummer: SI/501299 / 810003203

Summary

INFLOSCOM (IN-nozzle FLOw, Spray and COMbustion) is a four years industrial research project with the aim to better understand the mechanisms and relations between cavitation and spray breakup in large two-stroke marine Diesel engine fuel injectors. So far, there is only very limited knowledge available since most of the research on fuel injection is focused on automotive and heavy-duty engines. The fuel injection nozzles of large two-stroke marine Diesel engines differ extensively regarding their nozzle bore size and especially their completely non-symmetrical and eccentrical nozzle bore arrangement. A deeper understanding regarding the in-nozzle flow and especially cavitation within the nozzle is inevitable to further enhance the performance of such injection systems and hence, improve engine efficiency and reduce emissions, accordingly.

A newly developed transparent nozzle allows a qualitative visualization of the in-nozzle flow under real-size dimensions and with engine-like fuel pressure conditions. The study revealed a variety of steady-state and transient cavitation phenomena from different single-hole nozzle geometries investigated. Using hydro-erosive grinding, nozzles with different levels of inlet radii were studied as well and the qualitative in-nozzle flow data was linked to quantitative spray morphology and combustion results acquired at the Spray and Combustion Chamber (SCC) facility at Winterthur Gas & Diesel Ltd. (WinGD) in Winterthur, Switzerland.

The results show the significant reduction of cavitation and level of spray atomization with an increasing level of hydro-erosive grinding of the nozzles. Spray angles and deflections were evaluated and linked to the in-nozzle flow cavitation patterns to evaluate the dominant parameters and to further deepen the understanding of the nozzle orifice design and the influence on the resulting spray formation and morphology. CFD simulations were set up and successfully validated using the gathered experimental data revealing additional flow features and information about the in-nozzle flow.

The complete experimental data set generated in this project is facilitating the validation of spray and subsequent combustion simulations in the future development process within the R&D department of WinGD. The gained understanding of the cavitation behavior of nozzles will help to optimize the fuel injection process by adapting nozzle designs to compensate spray deflections and reduce nozzle wear induced by cavitation.

Take-home messages

- in-nozzle flow cavitation images revealing new details about Diesel fuel injection
- strong influence of nozzle geometries, especially using hydro-erosive grinding, on cavitation, spray formation and combustion
- linked spray morphology and combustion measurements allow quantifying the in-nozzle flow properties
- successful validation of in-nozzle flow CFD simulations with the experimental data acquired

Riepilogo

INFLOSCOM (IN-nozzle FLOW, Spray e COMbustion) è un progetto di ricerca industriale della durata di quattro anni con l'obiettivo di comprendere meglio i meccanismi e le relazioni tra cavitazione e spray breackup negli iniettori per grandi motori Diesel due tempi in ambito marino. Finora, le conoscenze disponibili sono molto limitate, poiché la maggior parte della ricerca sull'iniezione di carburante è focalizzata sui motori automobilistici e heavy-duty. Poiché gli ugelli di iniezione del carburante dei grandi motori marini Diesel a due tempi differiscono ampiamente per quanto riguarda le dimensioni dell'alesaggio degli ugelli e soprattutto per la loro disposizione completamente non simmetrica ed eccentrica del foro dell'ugello, è necessario acquisire una comprensione più profonda del flusso e della cavitazione all'interno dell'ugello per comprenderne l'influenza nella formazione dello spray e nella combustione, al fine di migliorare ulteriormente le prestazioni di tali sistemi di iniezione e di conseguenza l'efficienza del motore così come ridurre le emissioni.

Un ugello trasparente di nuova concezione permette una visualizzazione qualitativa del flusso all'interno dell'ugello di dimensioni reali e con condizioni di pressione del carburante simili a quelle del motore. Lo studio ha rivelato una varietà di fenomeni di cavitazione stazionaria e transitoria nelle diverse geometrie di ugelli a foro singolo indagate. Utilizzando la macinazione idro-erosiva, sono stati studiati anche gli ugelli con diversi livelli di raggio di ingresso e i dati qualitativi del flusso all'interno dell'ugello sono stati collegati alla morfologia quantitativa degli spruzzi e alla risultante combustione. Tutti i dati sono stati acquisiti presso l'impianto denominato Spray Combustion Chamber (SCC) Winterthur Gas & Diesel Ltd. (WinGD) a Winterthur, Svizzera.

I risultati mostrano la significativa riduzione della cavitazione e del livello di atomizzazione del getto con un livello crescente di macinazione idro-erosiva degli ugelli. Gli angoli di spruzzo e le deviazioni sono stati valutati e collegati ai modelli di cavitazione del flusso all'interno dell'ugello per valutare i parametri dominanti e per approfondire ulteriormente la comprensione del design dell'orifizio dell'ugello e la sua influenza sulla formazione di spruzzi e sulla morfologia risultante. Le simulazioni CFD sono state impostate e validate con successo utilizzando i dati sperimentali raccolti che hanno rivelato ulteriori caratteristiche del flusso all'interno dell'ugello.

L'insieme completo di dati sperimentali generati in questo progetto stanno facilitando la convalida delle simulazioni dello spray e delle successive simulazioni di combustione nel futuro processo di sviluppo all'interno del dipartimento di ricerca e sviluppo di WinGD. La comprensione acquisita del comportamento di cavitazione degli ugelli aiuterà ad ottimizzare il processo di iniezione del carburante, adattando il design degli ugelli per compensare le deviazioni di spruzzatura e ridurre l'usura degli ugelli indotta dalla cavitazione.

Zusammenfassung

INFLOSCOM (IN-nozzle FLOW, Spray and COMbustion) ist ein vierjähriges industrielles Forschungsprojekt mit dem Ziel, die Mechanismen und Beziehungen zwischen Kavitation und Sprayzerfall in grossen Zweitakt-Dieselmotor-Kraftstoffinjektoren für Schiffsmotoren besser zu verstehen. Bisher liegen nur sehr begrenzte Erkenntnisse vor, da sich die Forschung im Bereich der Kraftstoffeinspritzung hauptsächlich auf Automobil- und Schwerlastmotoren konzentriert. Die Kraftstoffeinspritzdüsen grosser Zweitakt-Schiffsdieselmotoren unterscheiden sich hinsichtlich der Grösse und insbesondere ihrer völlig unsymmetrisch und exzentrisch angeordneten Düsenbohrungen stark von herkömmlichen Kraftstoffeinspritzdüsen. Ein tieferes Verständnis der Strömung in der Düse und insbesondere der Kavitation sind unumgänglich, um die Leistung solcher Einspritzsysteme weiter zu steigern und damit den Wirkungsgrad des Motors zu verbessern und die Emissionen zunehmend zu reduzieren.

Eine neu entwickelte transparente Düse ermöglicht eine qualitative Visualisierung der Strömung unter realen Abmessungen und motorähnlichen Kraftstoffdruckbedingungen. Die Studie zeigt eine Vielzahl von quasi-stationären und transienten Kavitationsphänomenen aus verschiedenen untersuchten Einlochdüsengeometrien. Durch hydroerosives Schleifen wurden auch Düsen mit unterschiedlichen Einlassradien untersucht. Die qualitativen Daten der Düseninnenströmung wurden mit der quantitativen Spraymorphologie und den Verbrennungsergebnissen verknüpft, die in dem Prüfstand Spray and Combustion Chamber (SCC) der Winterthur Gas & Diesel AG (WinGD) gewonnen wurden.

Die Ergebnisse zeigen die signifikante Reduktion der Kavitation und des Zerstäubungsgrades des Sprays mit zunehmendem hydro-erosivem Schleifen der Düsen. Sprühwinkel und Auslenkungen wurden ausgewertet und mit den Kavitationsmustern der Strömung in der Düse in Verbindung gebracht, um die dominierenden Parameter zu bewerten und das Verständnis des Düsendesigns und des Einflusses auf die resultierende Spraybildung und -morphologie weiter zu vertiefen. CFD-Simulationen wurden durchgeführt und erfolgreich mit den gesammelten experimentellen Daten validiert. Die Simulationsergebnisse liefern zusätzliche interessante Strömungsmerkmale und Informationen über die Strömungsverhältnisse in der Düse.

Der vollständige experimentelle Datensatz der in diesem Projekt generiert wurde erleichtert die Validierung von Spray- und Verbrennungssimulationen im zukünftigen Entwicklungsprozess innerhalb der F&E-Abteilung von WinGD. Das gewonnene Verständnis des Kavitationsverhaltens von Düsen wird dazu beitragen den Kraftstoffeinspritzprozess zu optimieren indem die Düsendesigns so angepasst werden, damit sie Sprayablenkungen kompensieren und den durch Kavitation hervorgerufenen Düsenverschleiss reduzieren.

Table of contents

1 Introduction ... 8

1.1 Background ... 8

1.2 Methods ... 9

1.3 Objectives ... 10

2 In-nozzle flow investigations ... 11

2.1 Introduction ... 11

2.2 Experimental setup ... 12

2.3 Results ... 14

3 Spray investigations ... 17

3.1 Introduction ... 17

3.1.1 Ballistic Imaging ... 17

3.2 Experimental setup ... 17

3.2.1 Ballistic imaging ... 17

3.2.2 Simultaneous in-nozzle flow and spray imaging ... 18

3.3 Results ... 18

3.3.1 Ballistic imaging ... 18

3.3.2 Spray images ... 20

3.3.3 Spray morphology ... 20

4 Combustion investigations ... 24

4.1 Introduction ... 24

4.2 Experimental setup ... 24

4.3 Results ... 26

5 CFD validation ... 29

5.1 Introduction ... 29

5.2 Results ... 29

6 Discussion ... 33

7 Conclusions ... 34

8 Outlook ... 35

9 National and international collaboration ... 35

10 Dissemination ... 36

11 Publications ... 37

12 References ... 38

Abbreviations

SCC	Spray and Combustion Chamber
WinGD	Winterthur Gas & Diesel Ltd.
Chalmers	Chalmers University of Technology, Department of Mechanics and Maritime Sciences, Division of Combustion and Propulsion Systems
CFD	computational fluid dynamics
IMO	International Maritime Organization
EGR	exhaust gas recirculation
TNH	transparent nozzle holder
PMMA	polymethyl methacrylate
CMOS	complementary metal-oxide-semiconductor
ICU	injection control unit
nHG	non-hydro-erosive ground, viz. sharp-edged
HG	hydro-erosive ground
OKE	optical Kerr effect
SHG	second harmonic generation
SOI	start of ignition/injection
BI	Ballistic Imaging
FOV	field of view
RANS	Reynolds-averaged Navier-Stokes equations
uRNAS	unsteady Reynolds-averaged Navier-Stokes equations
OLP	optical light probe
VOF	volume of fluid method
LES	large eddy simulation
CERC	Combustion and Engine Research Center
PIV	particle image velocimetry

1 Introduction

1.1 Background

Winterthur Gas & Diesel Ltd. (WinGD) is a Swiss company that provides advanced two-stroke marine engine solutions. The engines are constructed by various licensees and installed in vessels at the shipbuilders. The main products are the solutions that are driven by R&D within the company; much of it by fundamental understanding, experimental investigations, and computational fluid dynamics (CFD). One of the greatest impediments to next-generation fuel injection systems in such engines is the ability to predict coupled spray formation, mixing, and combustion. The goals of this project are therefore to deliver the investigations required to develop new simulation models with experimental validation, accordingly.

Much of the ongoing marine engine development is focused on meeting the requirements of the International Maritime Organization (IMO) Tier III legislation which will first go into effect in 2016 and 2021. Tier III dictates an 80% reduction in NO_X engine out levels. Engine manufacturers are investigating engine internal NO_X reduction methods such as Miller/Atkinson timing, water-in-fuel emulsion, EGR, etc. The development of these methods requires that engine manufacturers have a detailed understanding of all the internal engine processes, including fuel injection processes and the subsequent spray formation and combustion. The challenge to CFD modeling of such engines is to achieve better predictability. There is a lack of knowledge regarding the flow in the interior of the nozzle, especially cavitation, and its effect on fuel spray formation (primary breakup). Primary breakup is the least understood part of the spray combustion process [1] [2]. It is becoming clear that cavitation plays an important role in the development of such an injection system. It can occur as *geometric cavitation* (located at the corner and wall of the nozzle hole and caused by the sudden reduction of static pressure as the flow enters the passages) or as *string cavitation* (sometimes called *vortex cavitation*, appearing transiently within the core of strong vortices that can build up in these geometries [3]. It appears that both types of cavitation can occur in the kind of injector under study. It is not clear how switching from one type of internal flow to another will affect spray formation and thus spray breakup, mixing, and combustion in a real marine two-stroke Diesel engine during one cycle.

To further optimize the large marine two-stroke Diesel engines, tools are necessary to support the development which enables optimization of brake specific fuel consumption and reduction of exhaust gas emissions in an efficient way to meet the upcoming legislation and to increase the competitiveness. Additionally, such models facilitate the reduction of testing time and therefore, directly reduce fuel consumption and CO_2, NO_X, and soot emissions (which is a non-negligible amount, considering the fuel consumption rate of several tons per hour).

In order to reduce costs and to increase reliability the trend in shipping goes towards larger vessels. The larger the ships are, the larger is the main engine which in turn is coupled to higher efficiency due to reduced wall heat losses and reduced friction in relation to the power output. Small and medium-sized Diesel engines have been investigated for decades and they are quite well understood in terms of emission formation and there are ways to prevent or reduce such emissions. In very large engines, effects become dominant which cannot be seen or have very limited influence in smaller or medium-sized engines that are heavily researched. Additionally, the positioning of the multiple fuel injectors of large marine Diesel engines is different: instead of a central mounting resulting in a symmetrical arrangement of the multiple nozzle bores, the multiple injectors of large two-stroke marine engines protrude the cylinder cover from the periphery and are arranged by 180° (two injectors for smaller engines) or 120° (three injectors for larger engines). This injector arrangement leads to a completely asymmetric and eccentric nozzle bore configuration in the nozzle tip.

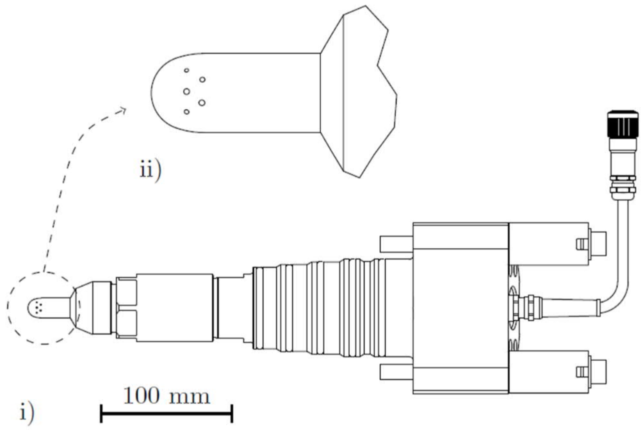

Figure 1: Illustration of a standard fuel injector with mounted nozzle tip (i) as used in large marine two-stroke Diesel engines and enlarged (4:1) detail of the nozzle tip (ii) [4].

Figure 1 depicts a schematic illustration of a typical fuel injector with a mounted nozzle tip (i) and an enlarged cut-out detail of the nozzle tip with its standard five nozzle bore design (ii). The beforementioned asymmetric nozzle bore arrangement is clearly visible as all of the five nozzle bores face a similar direction. This inevitable nozzle bore design leads to eccentrically arranged nozzle bores with respect to the nozzle main bore, which are not common in medium and small-sized combustion engines and as a result, there is a lack in experimental data to validate CFD simulations.

1.2 Methods

The aim of the project is the clarification of the in-nozzle flow influence, in particular cavitation, on the primary liquid breakup, spray morphology, and combustion under conditions relevant for large marine Diesel engines. Earlier experiments carried out in the Spray Combustion Chamber (SCC) at WinGD revealed effects that could not be further examined with conventional methods [5]. By making use of highly sophisticated optical measurement techniques, i.e. using transparent nozzles and ballistic imaging, INFLOSCOM shall answer questions about the processes in the spray nozzle and transfer the results into extended CFD models.

Chalmers University of Technology, Department of Mechanics and Maritime Sciences, Division of Combustion and Propulsion Systems (Chalmers), has recently developed optically transmissive injector tips that can withstand higher fuel pressures than former designs [6]. The experimental equipment and the technology behind it are modified to match with real-size nozzle geometries and used for the in-nozzle flow investigations. The spray formation in the near field can be observed using ballistic imaging, a state-of-the-art optical measurement technique for temporal spray investigations.

Unfortunately, rebounding fuel jets inside the spray and combustion chamber at Chalmers produced streams of large drops that filled the space between the jet and the window. Ballistic imaging can minimize image corruption by small drops that scatter light off-axis. Large drops in the geometric regime refract light without scattering, and so when present in high number density and when out of focus, they simply attenuate light. Moreover, the same jets then coated windows and caused further attenuation. As a result, the first project step is the development of an ambient temperature, pressurized chamber designed specifically for marine injectors. It will minimize the fuel jet rebound problem and improve the quality of the images. Ambient temperature will be used here so that transparent tips can be used in coordination with ballistic imaging. In the near field, the density ratio and cavitation number matter much more than temperature, and it will be possible to match important density ratios and cavitation numbers at ambient temperature.

The far-field of the spray under combusting and non-combusting conditions will be investigated using the high pressure and temperature, constant-volume spray chamber SCC at WinGD in Winterthur. This chamber has the same cylinder bore as a conventional marine two-stroke engine. The swirl flow in such engines is also emulated by hot gas entering the combustion chamber from the heater section (regenerator). In this device, the gas pressure can peak at 200 bar with temperatures of more than 900 K. Windows can be located at various positions allowing investigators to view different regions of the spray and flame. High-speed planar laser diagnostics are available for Mie scattering from drops, Rayleigh scattering from molecules, and selected laser induced fluorescence methods. Injector concepts that have been investigated in optical layouts at Chalmers will subsequently be investigated as metal injectors at WinGD for a full accounting of spray performance from inside the injector all the way out to a burning tip.

1.3 Objectives

The goal of the project lies in the clarification of the influence of the in-nozzle flow, especially cavitation, on the spray development and the combustion under conditions as they can be found in large marine two-stroke Diesel engines. Investigations at the SCC revealed effects that could not be further examined with conventional methods within the European Union funded HERCULES-C project [5]. By making use of highly sophisticated optical measurement techniques, INFLOSCOM shall answer questions about the processes in the spray nozzle and transfer the results into existing CFD models.

The following project objectives have been set:
- to identify and characterize the major influences of the in-nozzle flow on primary breakup and spray morphology
- investigation of the cavitation in the nozzle by means of optically accessible transparent nozzles
- investigation of possible applicability of PIV in transparent nozzles
- visualization of the surface structure exiting the nozzle by means of ballistic imaging and quantification of the structure during the quasi-steady-state injection period
- development of (phenomenological) models to describe the effects seen in the above investigations
- transfer cavitation investigations to SCC and visualize the influence of the different flow conditions on spray morphology (spray angle and penetration) and combustion (ignition spot and flame development) under engine relevant condition as a basis for the final model tuning
- analysis of the cavitation noise in the frequency domain (→ make conclusions of cavitation size/intensity to develop a sensor for non-transparent nozzles)

In scope:
- quantification of the position, size, and shape of the cavitation pockets, eventually as a function of time
- description of the shape and surface of the spray close to the nozzle during the stable phase
- determination of the influence of selected parameters on cavitation and spray surface
- improvement of existing models and implementation of cavitation phenomena in order to increase the precision of the simulation tools

Out of scope:
- influence of cavitation on nozzle lifetime
- quantitative determination of flow velocities in the nozzle or in the field near to the nozzle
- ballistic imaging in the engine or the SCC

2 In-nozzle flow investigations

2.1 Introduction

The fuel injection process in modern Diesel injectors is performed using nozzles of small diameters at high rail pressures to enhance the aerodynamic breakup of the fuel spray in order to provide a sufficient level of fuel atomization. Cavitation is an essential attribute of the flow under such conditions [7] [8]. As a result, the optimization of the injection process requires eliminating or understanding and reliable prediction of cavitation.

Cavitation is the process of formation and consequent collapse of gaseous bubbles in a liquid under a local decrease in static pressure. Depending on the topology of the vapor structures in the flow, cavitation occurs in a form of traveling bubbles, or vapor pockets, extending over a partial length of the nozzle bore (*cloud cavitation* and *sheet cavitation*), or *supercavitation*, when the vapor region extends over the whole length of the nozzle bore [9].

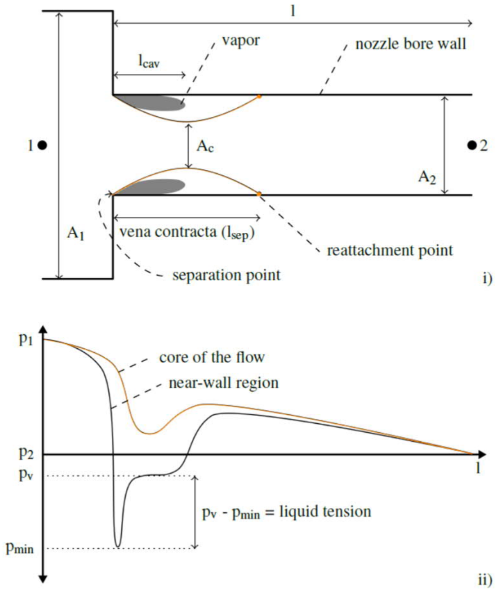

Figure 2: Theoretical geometry induced cavitation i) and pressure variation ii) in an atomizer with the liquid flowing through the main bore (1) with diameter A1 entering the nozzle bore with diameter A2 and leaving at the nozzle bore exit, also called orifice (2) into the plenum [10].

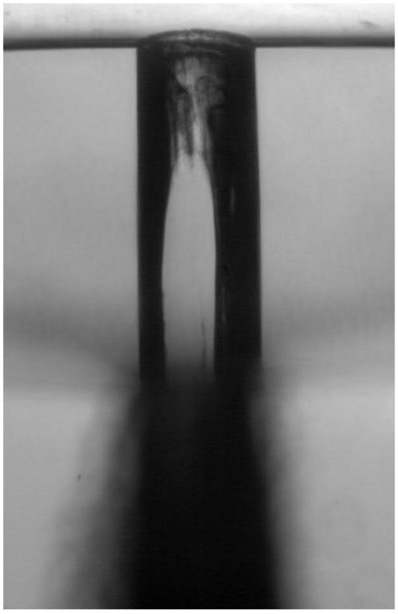

Figure 3: Shadowgraph of in-nozzle flow using a transparent nozzle. Dark pixels indicate cavitation, geometry boundaries, or spray. The vertically arranged nozzle bore has a diameter of 0.75 mm and the exit of the nozzle bore approximately in the vertical middle of the image indicates the emerging of the spray [11].

Hydrodynamic cavitation in fuel injectors occurs at high injection rates when the pressure drops below the critical level inside the nozzle bore, leading the fuel to suddenly evaporate. When the pressure reduction is caused by a sudden change in the geometry of the stream, the flow tends to separate and form a *vena contracta* inside the beginning of the nozzle bore; geometry-induced cavitation occurs. Figure 2 i) depicts a schematic of a nozzle geometry with a typical vena contracta and the resulting reduced area A_c. The contraction from the nozzle main bore (1) into the nozzle bore reduces the cross-section area from A_1 to A_c. This area reduction leads to a velocity increase and a pressure depression in the throat of the nozzle as shown with the pressure along the nozzle depicted in Figure 2 ii). At the nozzle bore inlet, a recirculation zone can be observed with a separation and reattachment point defining the length of the *vena contracta,* l_{sep} (compare with schematic depicted in Figure 2 i)). When the local pressure inside the nozzle drops below the vapor pressure of the liquid p_v, hydrodynamic cavitation occurs. Pressure waves traveling through the fluid domain can cause pressure reduction leading to dynamically induced cavitation [12]. Cavitation is reported to improve the spray breakup processes [8] [13] [14] [15] [16], however other undesirable effects on the fuel injection performance may occur such as increased nozzle material wear.

First data has been acquired using an existing transparent nozzle holder (TNH) developed at Chalmers. However, due to the limited size (half-scaled) and different geometry not matching real-size fuel injector nozzles of WinGD injectors, a new TNH has been developed. A typical in-nozzle flow image as acquired in this project is depicted in Figure 3. The image has been taken at a rail pressure of 500 bar using a high-speed camera and a laser diode background illumination. As a result, cavitation is indicated as dark areas since the light is refracted at the gaseous phase. Note that the spray emerges from the exit of the nozzle bore at the bottom half of the image. The experimental setup leading to those images is described in the next chapter.

2.2 Experimental setup

Transparent nozzles made from polymethyl methacrylate (PMMA) were used to visualize the in-nozzle flow of large marine two-stroke Diesel engines injectors. PMMA was chosen due to its refractive index which roughly matches Diesel fuel and its superior pressure resistance compared with quartz glass [6]. Due to the cylindrical design of the injector nozzle bores it is necessary to use refractive index matching since the orifice shape acts as a lens distorting the light used for optical measurements. To cope with the high fuel pressures during the quasi-steady-state injection process, the transparent nozzle is braced in a so-called transparent nozzle holder (TNH). External forces are applied from all sides to the rectangular-shaped PMMA nozzle as investigations have shown that this decreases the failure probability significantly [6].

The nozzles used in this project are single-nozzle bore designs to save computational cost of the CFD simulations. Additionally, multi-hole configurations would further weaken the PMMA nozzles and disturb the optical access for line-of-sight optical methods. The nozzle bore diameter is 0.75 mm and the main bore diameter 3.5 mm which are representative dimensions for large marine Diesel engine injector nozzle tips. Three different nozzle configurations have been chosen based on realistic geometrical properties of the injector tips:

- N101: orthogonal, centrically arranged nozzle bore
- N104: orthogonal, eccentrically arranged nozzle bore
- N105: angled, centrically arranged nozzle bore

The schematic illustrations of the three nozzles used are depicted in Figure 5. These transparent nozzles are mounted in the TNH which is illustrated in Figure 4 with a top view (a), a side view (b), and a sectional view detail showing the PMMA nozzle with the main bore and nozzle bore (c). The whole TNH is mounted on a WinGD injector using the standard mount from a conventional nozzle tip (8). The PMMA nozzle is sealed using standard O-rings with a hardness of 90 Shore-A. A piezoresistive pressure sensor (Kistler 4067C2000) is mounted as close as possible to the transparent nozzle without a tap that can decrease the frequency spectrum due to Helmholtz-resonator effects. The sensor used has a natural frequency of over 200 kHz that allows dynamic pressure data acquisition. The PMMA nozzle is pressed together by the main body (8) and the body that holds the pressure sensor. Additionally, two clamps mounted on top of the TNH (3) and two clamps on the side (2) apply a defined force to the nozzle's other surfaces. Due to optical access, the side clamps (2) apply the force via polished sapphire bricks (4). Sapphire was chosen due to its excellent optical and tensile strength properties. The two sapphire bricks (4) together with the side clamps (2) allow the application of line-of-sight optical measurements. Due to this compression of the PMMA nozzle, it is possible to apply realistic marine two-stroke Diesel engines injection pressures. However, the PMMA construction can only withstand a limited number of injections before it fails.

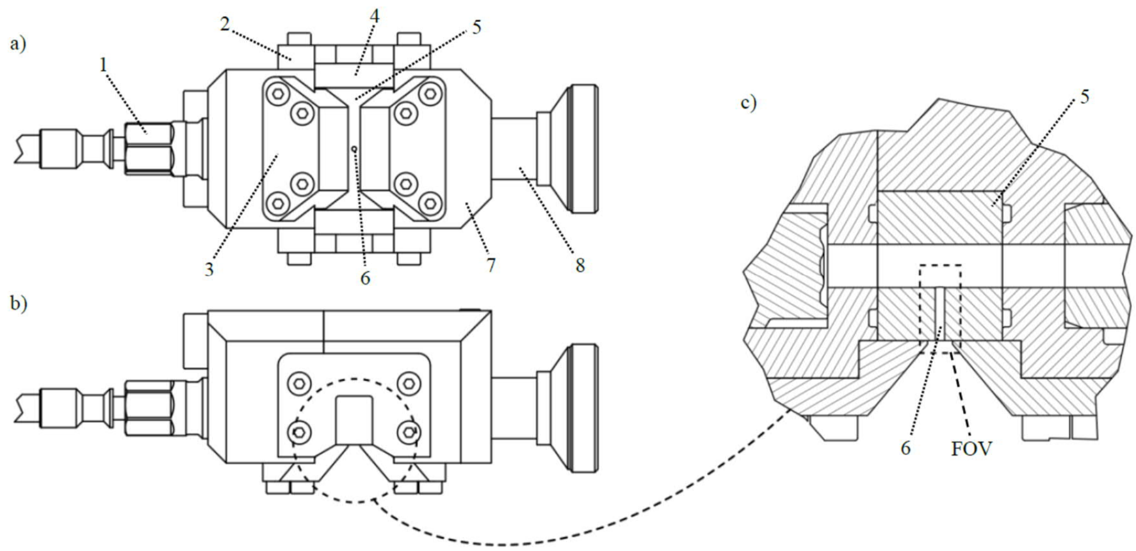

Figure 4: Schematic of transparent nozzle holder: top (a) and side (b) view and sectional view of transparent nozzle (c) with pressure sensor (1), side clamp (2), top clamp (3), sapphire brick (4), transparent nozzle (5) with orifice (6), main body (7) and injector mount (8). The sectional view (c) also depicts the approximate location of the used field of view (FOV) of the optical measurements [17].

The in-nozzle flow is imaged using pulsed-light shadowgraphy. The optical setup is depicted in Figure 6 and consists of a far-field microscope (Questar QM100) (b) and a CMOS high-speed camera (Photron Fastcam HSS6) (a). A pulsed, diode laser (Cavitar Cavilux Smart) (i) together with a collimator optic (g) and a focusing lens (f) were used as an illumination source. To guarantee a uniform background illumination, a diffusor plate (e) has been mounted before the spray chamber optical window. To acquire sharp images, a pulsed light source is necessary to reduce motion blur given that the velocities in the orifice are in the order of 300 m/s.

The fuel used in this project is a commercially available Diesel with a density of 815.9 kg/m^3 (at 20° C) and a viscosity of 2.112 mm^2/s (at 40° C). The fuel was pressurized using a high-pressure, air-driven liquid pump (Haskel DSXHF-452) together with a 5 dm^3 piston accumulator to stabilize the fuel pressure. The rail pressure was 500 bar and the back pressure was ambient atmosphere. The injection duration was set to 12 ms. For the experiments performed at the SCC at WinGD, the identical conditions were used, however, a Diesel rail together with an injection control unit (ICU) as used on WinGD's engines was used as fuel delivery system. A media separator (developed for the BFE funded project 154269/103241) was installed between ICU and injector to allow using the identical Diesel fuel as used for the measurements performed at Chalmers.

The optical setup as depicted in Figure 6 is slightly altered between the different experimental campaigns (different high-speed cameras and light sources) but the working principle of the Shadowgraphy optical measurement technique remains identical.

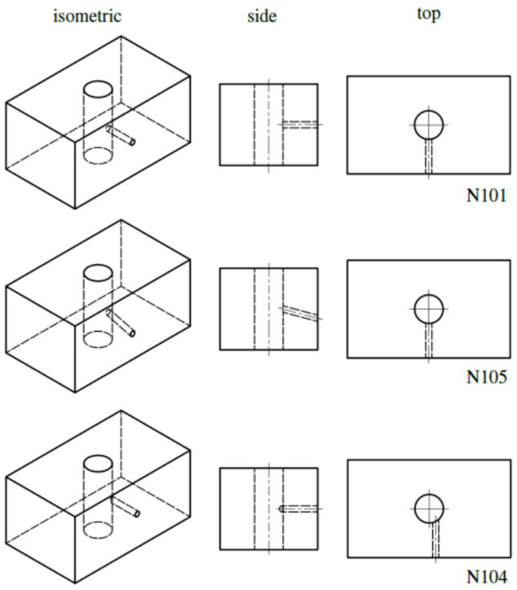

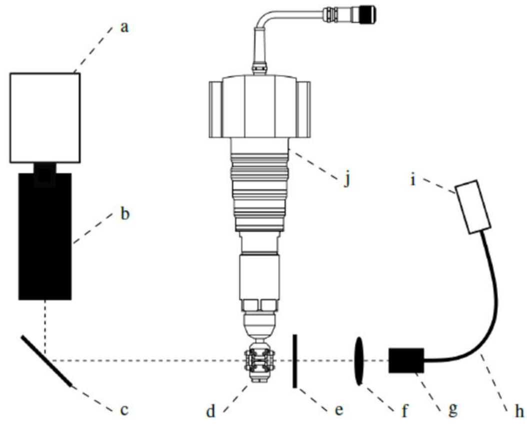

Figure 5: Isometric, side, and top projection of the three different transparent nozzle types used. N101: centrically arranged 90° setup, N105: centrically arranged 75° setup and N104: eccentrically arranged 90° setup. The main bore diameter is 3.5 mm and the nozzle bore diameter is 0.75 mm [18].

Figure 6: Schematic of the optical setup used with high-speed camera (a), far-field microscope (b), mirror (c), transparent nozzle holder (TNH) (d), diffuser plate (e), focusing lens (f), collimator (g), optical fiber (h), diode laser (i) and injector (j). The dashed line represents the optical axis. Note that the spray chamber surrounding the TNH is not illustrated [18].

The first in-nozzle flow images acquired under realistic injection conditions revealed a very distinct level of cavitation (see Figure 3). It became clear that the nozzles need to be flow-optimized as common for commercial injector nozzles to better match WinGD nozzle geometry requirements. As a result, a hydro-erosive grinding rig has been developed and built. With this rig, the transparent PMMA nozzles and later on the metallic nozzles could be flow-optimized by inducing inlet radii between main and nozzle bore which as a consequence reduces cavitational flow.

2.3 Results

The first in-nozzle flow images acquired at Chalmers and depicted in Figure 3 and Figure 7 used a shortened version of the nozzle design N101 as illustrated in Figure 5. The field of view used in the in-nozzle flow images depicted in Figure 7 is illustrated in the schematic of the TNH in Figure 4. The nozzle is *supercavitating* as the geometrical cavitation extends over the whole length of the nozzle bore. The flow is entering the nozzle bore through the horizontally arranged main bore from the right side, hence the geometrical cavitation is larger on the right side of the nozzle bore due to stronger flow deflections. Note that the cavitation is very strong since the nozzle is sharp-edged. At the nozzle bore entry, the geometrical cavitation spans over the whole circumference of the nozzle bore. Although significantly weaker in the optical axis, it is clearly visible that the cavitation pockets extend until approximately a third of the nozzle bore length before they disintegrate and allow the light to pass the center of the nozzle bore without disturbances.

These first experimental images of the in-nozzle flow revealed the occurrence of different cavitation patterns: Geometrical cavitation on the nozzle bore walls which remains very steady during the quasi-steady state fuel injection process (see Figure 7 a)) and additional, more transient cavitation phenomena such as *string cavitation* (see Figure 7 b)) and *cloud cavitation* (see Figure 7 c)).

Due to the very strong cavitation patterns with the sharp-edge nozzle designs, the transparent nozzles where hydro-erosive ground for different amounts of time to further investigate the in-nozzle cavitational flow. The basic effect of hydro-erosive grinding is visualized in Figure 8 where a detail of a sharp-edged N101 nozzle bore (a) is shown using a microscope. The markings of the manufacturing are still visible as a spiral pattern on the nozzle bore walls. In addition, a strongly hydro-erosive ground N101 nozzle bore (b) indicates the inlet radii between main and nozzle bore and a very asymmetric nozzle bore entry. The also enlarged nozzle bore diameter is clearly visible and as a result, all the manufacturing marks are gone.

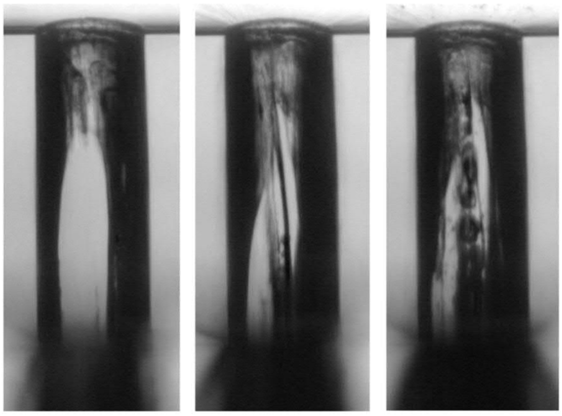

a) b) c)

Figure 7: Different cavitation phenomena: steady-state geometrical cavitation (a), unsteady string cavitation (b), and unsteady cloud cavitation (c).

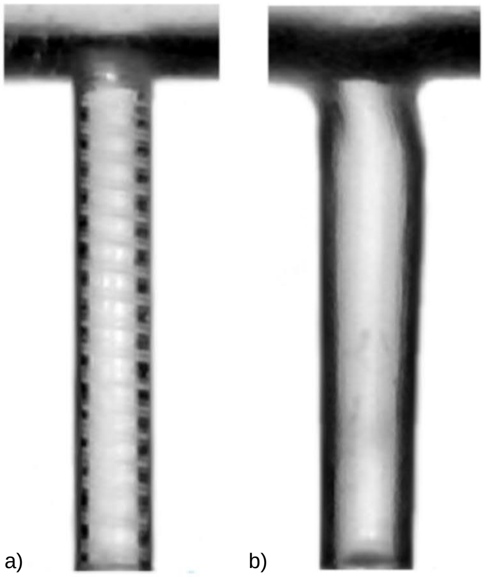

a) b)

Figure 8: Sectional view of microscope images of original (a) and hydro-erosive ground (b) transparent PMMA orifices.

The effect of flow optimization due to hydro-erosive grinding is depicted in Figure 9. The image a) shows a non-hydro-grinded (nHG) nozzle bore of an eccentrical N104 nozzle filled with fuel, but there is no flow. As a result, the walls of the main and nozzle bore are visible as dark lines, but no cavitation is occurring. The walls are visible since the refracting indices of the PMMA and the Diesel used are not perfectly identical, however, the image serves as a background reference. The next image to the right (b) shows the identical nozzle nHG, but at a rail pressure of 500 bar. Note that the flow is averaged by taking the average of the pictures acquired during the quasi-steady-state fuel injection. This applies to all images in Figure 9. The nozzle is *supercavitating*, but due to the eccentrical arrangement of the nozzle bore, the pattern is completely different from a non-eccentrical nozzle (compare with Figure 7). Although the nozzle bore seems fully cavitating, it can hardly be seen that the walls of the nozzle bore on the left and right side show no geometrical cavitation. By going to the next image on the right (c), hydro-erosive grinding has been applied and the non-cavitating walls are a bit stronger visible. By further increasing the level of hydro-erosive grinding (HG), the cavitation pattern significantly changes towards a swirl motion (between the images d) and e)) which is further enhanced with additional HG. The level of cavitation, in general, is reduced as well with an increasing level of HG. The image on the right (g) shows the maximal level of HG that was achievable before the PMMA nozzles failed. Unfortunately, it was not possible to HG the nozzles to a level where cavitation effects completely disappear at a rail pressure of 500 bar.

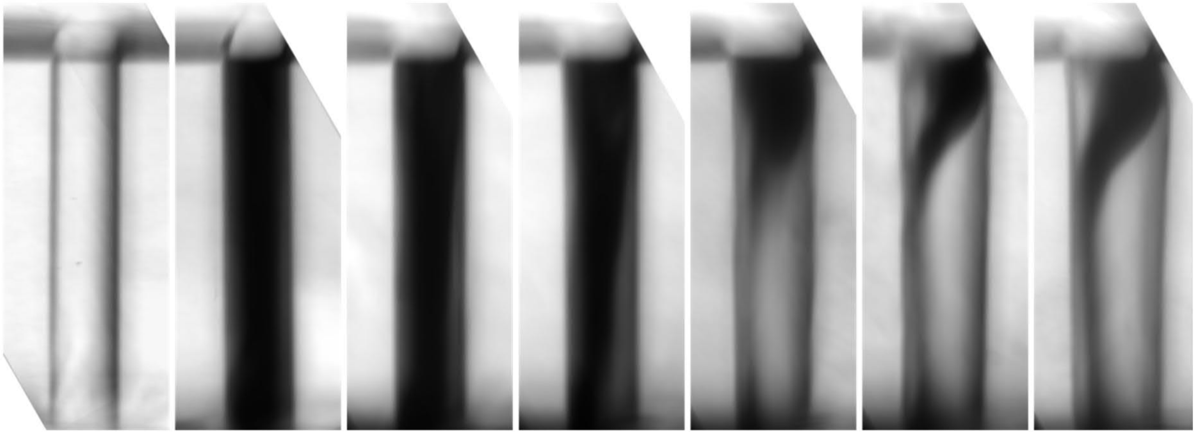

Figure 9: Averaged in-nozzle flow images of the nozzle N104 with different levels of hydro-erosive grinding (from left to right). The image far left indicated the background, since no fuel pressure is applied [19].

Although the in-nozzle flow images were acquired using high-speed cameras, the data can only be presented qualitatively. This is mainly due to the large fluid velocities in the nozzle bore and the limited frame rates of the high-speed cameras and frequencies of the light sources used. With the typical 20 kHz framerate used to record the in-nozzle flow, a time of 50 µs passes between two consecutive frames. In this time amount, the fluid flow moves roughly 10 to 15 mm. Note that the nozzle bore has a length of approximately 4.25 mm. As a result, local velocities of the in-nozzle flow could not be evaluated with the experimental equipment available. However, the qualitative in-nozzle flow data has been recorded simultaneously together with high-speed images of the spray emerging from the nozzles. This allows linking the qualitative in-nozzle flow images to quantitative spray morphology data evaluated from the spray images acquired.

3 Spray investigations

3.1 Introduction

The first spray investigations could be performed after an ambient temperature, constant-volume spray chamber for pressures up to 40 bar has been developed and built at Chalmers. Ballistic imaging, a state-of-the-art optical method, was applied to investigate the primary breakup region of the spray with matching conditions to the previously acquired in-nozzle flow images. The hardware, however, limited the acquisition rate to one spray and one in-nozzle flow image per injection. As a consequence, a more detailed, additional spray investigation measurement series using more standard optical measurement techniques as for example Shadowgraphie and OH*-chemiluminescence has been performed in the second project phase at the SCC at WinGD.

3.1.1 Ballistic Imaging

Ballistic imaging (BI) is a laser-based optical measurement technique to resolve structures in highly scattering media as for example dense fuel sprays. The technique is Shadowgraphy based as it is a line-of-sight method that eliminates multiply scattered light from the detector. The technique's aim is to reveal details of something surrounded by light scattering particles (e.g. fog, mist, smoke, etc.) which are disturbing the view. To obtain high-resolution spatial data in highly scattering media, BI limits the light collection by discarding photons that are heavily scattered. Therefore, only a small number of photons from the initial laser pulse are detected and evaluated on the high-speed camera. The name of the measurement technique comes from the term ballistic, which is referred to as photons that travel through a turbid medium without any scattering interaction.

As BI is a time-gated method, a very fast shutter (an optical Kerr effect (OKE) gate, based on CS_2) is used in front of the camera to discard the photons that are unwanted in the images.

3.2 Experimental setup

3.2.1 Ballistic imaging

Figure 10 depicts the schematic of a ballistic imaging optical setup used at Chalmers to acquire spray images. The spray chamber built with the WinGD injector mounted was placed exactly at the object plane. The BI setup chosen was a co-linear, two-color setup. In a typical co-linear setup as also described in [20], a high-frequency mode-locked laser which creates 50 to 150 fs pulses at a wavelength of 800 nm is used together with an amplifier as the light source. The beam is split into two beams using a 90/10 beamsplitter, one for triggering the OKE gate (switching beam, 90%), and one for the illumination of the spray (imaging beam, 10%). The switching beam uses a delay arm to set the temporal overlap of the two beams. This allows the exact triggering of the OKE gate. The imaging beam passes a half-wave plate and Glan-Thompson polarizer to adjust the light intensity before being frequency doubled using a second harmonic generation (SHG) nonlinear crystal. The light pulse with now 400 nm wavelength is guided through the object plane before passing the optical imaging configuration. The image configuration depicted in Figure 10 is a 4f-setup which is described in more detail in [21]. The imaging beam passes a two-lens setup for imaging purposes and in between the two lenses, two crossed Glan-Thompson polarizers, the OKE gate, and two dichroic mirrors are placed. The two short-pass dichroic mirrors are used to guide the switching beam through the OKE gate and removing it afterward from the optical path towards the camera. The switching beam intensity can be adjusted using another half-wave plate and polarizer setup. The additional half-wave plate in the switching beam path is used to optimize switching beam polarization to enhance the Kerr effect in the gate.

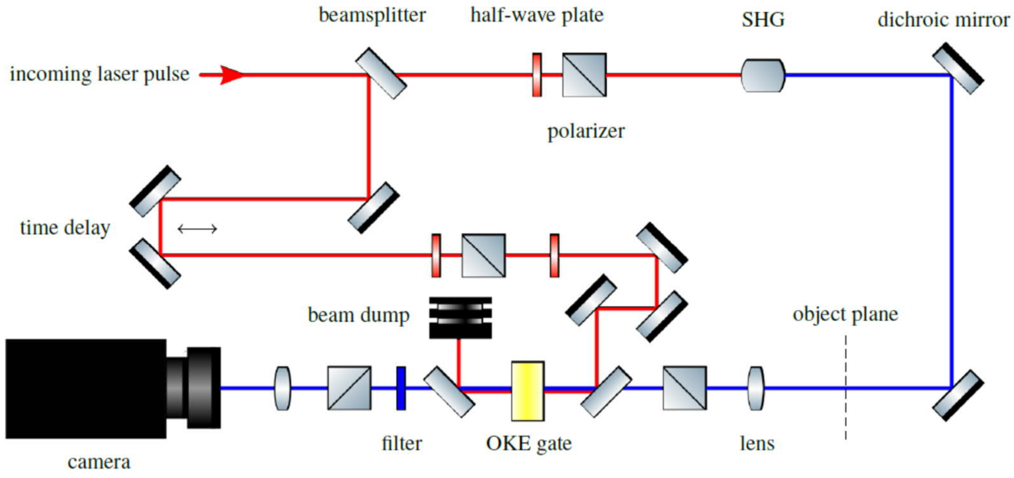

Figure 10: Schematic of time-gated, co-linear ballistic imaging setup. Note that the laser light source is not depicted in the schematic [10].

The polarized imaging beam passes the OKE gate where due to the nonlinear Kerr effect, the polarization is changed. This polarization change allows the imaging photons to pass the second polarizer and consequently the second imaging lens to hit the camera detector. If the switching beam does not trigger the Kerr effect in the OKE gate, the imaging beam's polarization does not change and the photons cannot pass the second, crossed polarizer. The first polarizer in the imaging configuration is used to well-define the polarization of the imaging beam before transmission to the OKE gate. The object plane shown in the schemata in Figure 10 indicates the position of the optical plane where the spray images have been acquired. The whole optical setup takes the spray chamber and its thick windows into account as well as the reduction of the speed of light and the consequent variation of the time delay. The technique was used to investigate the primary breakup of the spray by visualizing the spray close to the nozzle bore exit.

3.2.2 Simultaneous in-nozzle flow and spray imaging

In addition to the BI performed at Chalmers during the first project phase, simultaneous in-nozzle flow and spray images were acquired at the SCC in Winterthur in the second phase. Borrowing optical measurement equipment from WinGD's longtime research partners (ETHZ, PSI, EMPA, and FHNW) in Switzerland allowed the setup of high-speed image acquisition for both, in-nozzle flow and spray morphology measurements. The setup used is identical to the one presented in Figure 6, but an additional Shadowgraphy setup has been positioned. The second optical setup used a zoom lens instead of a far-field microscope and the second diode laser illuminated a larger area, allowing the acquisition of the spray images only limited by the maximal optical access diameters provided by the SCC. The detailed optical setup is described in more detail in [19].

3.3 Results

3.3.1 Ballistic imaging

Typical single-shot images acquired using time-gated BI are depicted in Figure 11. The dark area represents the spray which is emerging from the nozzle bore exit on top of the image and flowing downwards. As BI is an optical, line-of-sight measurement technique, the dark areas form because the light could not pass the spray and hence no signal arrived on the camera chip. The background of the images is typical for ultra-short pulse images showing aperture and interference patterns. The two images shown in Figure 11 a) and b) represent a typical acquisition during the quasi-steady state fuel injection at 5 ms after the start of injection (SOI) when the rail pressure is approximately constant (quasi-steady-state fuel injection). The two images are from nozzles with different inlet radii. Figure 11 a) shows the spray of a nozzle with sharp-edges at the nozzle bore inlet. The second nozzle which was used to create the image depicted in Figure 11 b) was slightly hydro-erosive ground and as a result, has a higher discharge coefficient. There is a significant difference in the spray breakup between a non (a) and a hydro-erosive ground nozzle (b) which can be seen in the spray cone: the cone angle in Figure 11 a) is significantly wider compared to the one in Figure 11 b). This is due to stronger cavitation in the nozzle, resulting in a more turbulent in-nozzle flow which widens the spray cone angle due to enhanced atomization.

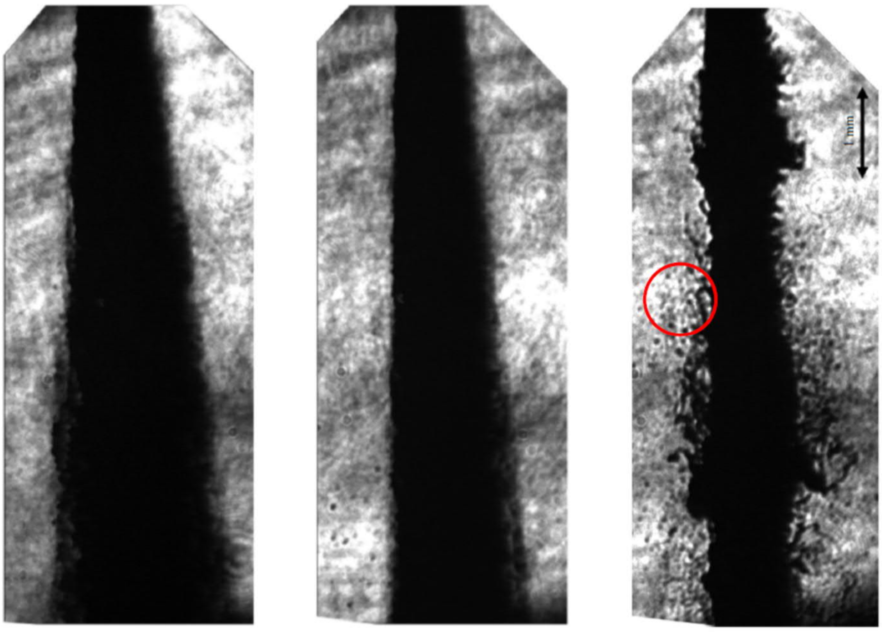

a) b) c)

Figure 11: Ballistic images of fuel spray emerging from the nozzle for different hydro-erosive ground nozzles with different discharge coefficients during quasi-steady-state fuel injection (a) 0.59, b) 0.74) and during the transient state of needle opening (c). The nozzle exit is located on top of the images (not visible) and the spray emerges towards the bottom [10].

The BI results depicted in Figure 11 a) and b) show no presence of large fluid structures such as voids, ligaments, blobs or droplets at the edge of the spray, which indicates that the spray in the near-field is dominated by a mostly intact liquid core and large droplets with limited separation and air entrainment. Figure 11 c) shows a spray acquired during the transient nozzle flow when the needle in the injector is lifting, 0.5 ms after SOI. At the spray breakup mechanism, structures can be clearly observed with a periodic as well as chaotic nature. Comparing the spray image from Figure 11 b) and c) reveals that the spray breakup process can be visualized in more detail during the transient, low-pressure phases occurring while the needle is opening. Also, the image in Figure 11 c) shows small droplets and ligaments which indicates that they would be resolved by the optical system in Figure 11 a) and b) if they were present (see red circle in Figure 11 c)). There are small spray breakup structures such as droplets and ligaments as well in Figure 11 a) and b) but they are too small and therefore cannot be detected as the resolution of the optical system is too low.

This limitation in spatial resolution together with the field of view limitation due to the optical components and the complexity of the optical setup lead to the conclusion that the optical measurement technique BI is only limitedly useful to investigate the sprays of large two-stroke marine Diesel engine fuel injectors under realistic geometrical and fuel pressure conditions. As the images are basically only qualitative data as well due to the distortion nature of the ballistic photons and the limited time gate opening time, the spray images acquired using BI are of little use to enhance the understanding of how the in-nozzle spray influences the spray breakup and morphology.

3.3.2 Spray images

The spray images acquired using high-speed Shadowgraphie with a frame rate of 20 kHz were evaluated for the standard spray morphology parameters. Selected edited images (adjusted background level, rotation, and segmentation) are depicted in Figure 12. The six sprays showed represent single shots taken during the quasi-steady-state fuel injection of the three different nozzles N101 (c), N105 (b), and N104 (a). The left spray image is from the sharp-edged nozzle while the right image is from the HG nozzle. As the sprays are leaving the optical access area, the top sides of the spray images depicted in Figure 12 are cut off by the window.

Figure 12: Spray visualization matching the in-nozzle flow: centrically arranged 90° orifice (N101) (c), centrically arranged 75° orifice (N105) (b), and eccentrically arranged 90° orifice (N104) (a). The left image shows the spray formation from the sharp-edged nozzle and the right image from the hydro-erosive ground nozzle configuration. The lower part of the sprays is cut-off due to the optical access limitations of the spray chamber. The nozzle bore exit is at the bottom of the images and the spray emerges towards the top. Note that the spray images from the angled nozzle (N105) have been rotated by 15° to enhance visualization.

The spray images shown in Figure 12 a) match the in-nozzle flow images shown in the previous chapter in Figure 9, however, those are averaged while the spray images are single shots. Nevertheless, the qualitative spray morphology changes are significant, especially strong for the eccentric nozzle N104 (a). The evaluated, quantitative information of the spray images is described in more detail in the next chapter.

3.3.3 Spray morphology

Various spray morphology values were evaluated using the edited spray images of the three different nozzles with their different HG levels. However, to define the quasi-steady-state fuel injection period, the evaluation of the in-nozzle fuel pressure is inevitable. The schematic in Figure 4 depicts the position of the pressure sensor used (1). The averaged and filtered in-nozzle pressure data of the eccentric nozzle N104 is shown in Figure 13. After approximately 2 ms after the electric start of injection (trigger), the pressure in the main bore of the nozzle starts to build up. The delay is due to the inertia of the needle movement. Note that the injection duration was set to 12 ms. The different pressure curves clearly show a trend towards lower maximal pressure and delayed rising time with further HG. This can be explained with the significant improvement of the flow characteristics which are caused by the hydro-erosive grinding process. Another indication of the reduced flow resistance with increasing level of HG are the more smooth pressure curves (compare *N104 noHG* with *N104 HG vi* in Figure 13) and the earlier pressure decrease at the end of the injection.

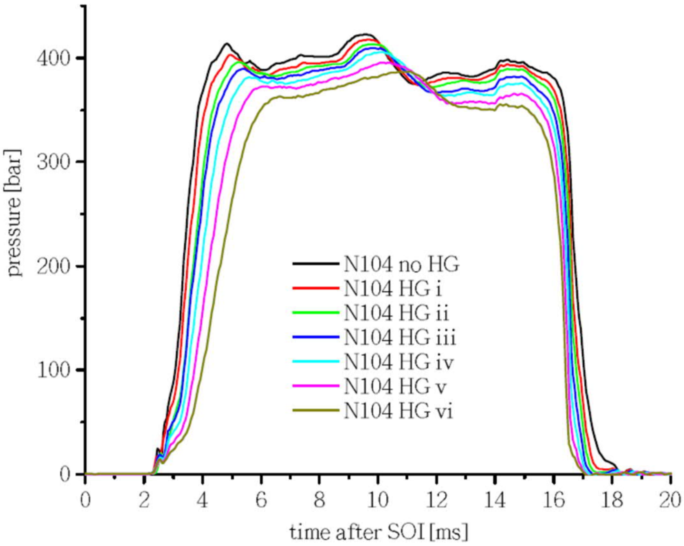

Figure 13: Averaged and filtered in-nozzle fuel pressure of the nozzle N104 for various levels of hydro-erosive grinding [19].

Although the pressure fluctuations after the needle opening are pronounced, their similarity over the different levels of HG is significant. The unsteadiness of the pressure are induced by the hydraulic system of the fuel preparation (high-pressure pump, rail, ICU, media separator, pipes), but as the fluctuations are still within decent standard deviations, a quasi-steady-state period form 6 to 15 ms after start of injection (SOI) has been selected and applied for the spray morphology evaluations.

Using this quasi-steady-state injection period, the spray contours could be averaged. A typical dataset is depicted in Figure 14. The plot shows the sharp-edged nozzle N104 and the maximal HG equivalent. The dotted lines indicate the standard deviation. As already visible in the single-shot spray images depicted in Figure 12 a), the spray of the eccentric nozzle N104 opens up massively. Additionally, it seems that the liquid spray core tends towards the left side and there is an enhanced vapor phase on the right. This effect can be seen more clearly in Figure 12 a) and is also represented with the much larger standard deviation on the right side in Figure 14. The spray from the HG nozzle is also much less symmetrical and the strong swirl cavitation flow as depicted in Figure 9 g) explains the sudden widening right after the exit of the nozzle bore exit. The comparatively small standard deviation justifies the use of the quasi-steady-state period. The significant spray angle changes are also depicted in Figure 15 over a wider range of levels of HG where they are fitted using a polynomial function for better comparison between the three different nozzle types. Note that the mass flow on the x-axis represents the different levels of HG: the mass flow increases with the intensity of HG due to reduced flow resistance and increases in nozzle bore diameter.

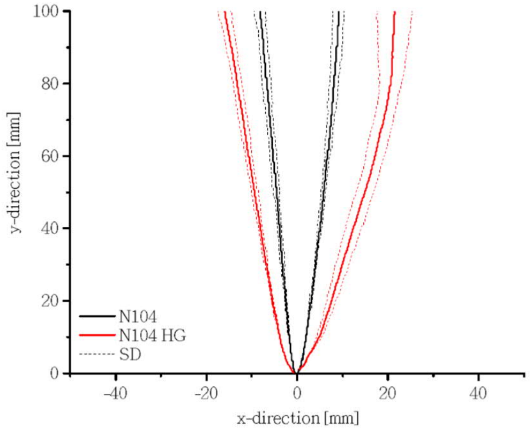

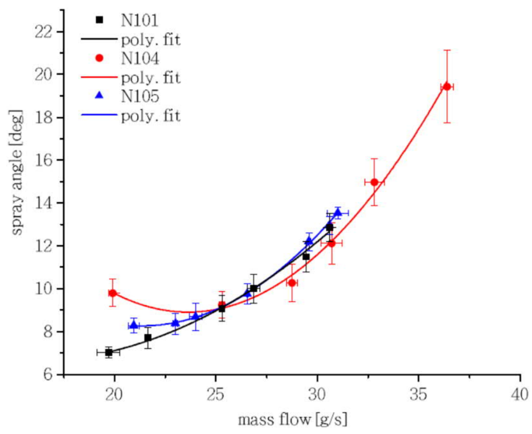

Figure 14: Averaged spray contours of the nozzle type N104 for sharp-edged (black) and hydro-erosive ground (red, HG) nozzles [19].

Figure 15: Spray angles of the three nozzle types for various hydro-erosive grinding levels [19].

The plot indicates that the nozzles N101 and N105 have a similar spray formation characteristic than the eccentric nozzle type N104. It is assumed that the strong in-nozzle swirl cavitation motion as depicted in Figure 9 leads to a significantly enhanced spray atomization and therefore a wider spray angle. The spray axis varies as well with increasing HG of the nozzles. Figure 16 depicts the spray axis changes of the three nozzle types investigated. Note that the horizontal dashed line represents the symmetrical axis of the noHG nozzle bores and that it is normalized for the angled N105 nozzle. The measurement points are connected for readability reasons.

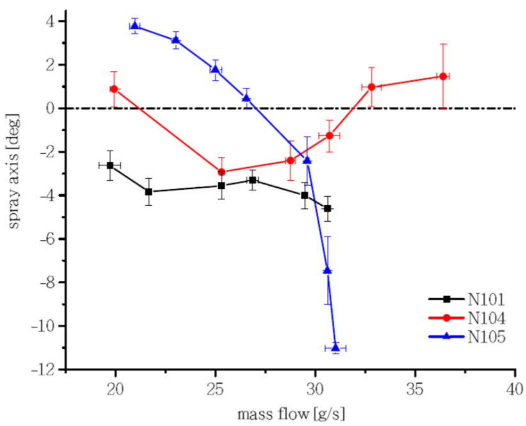

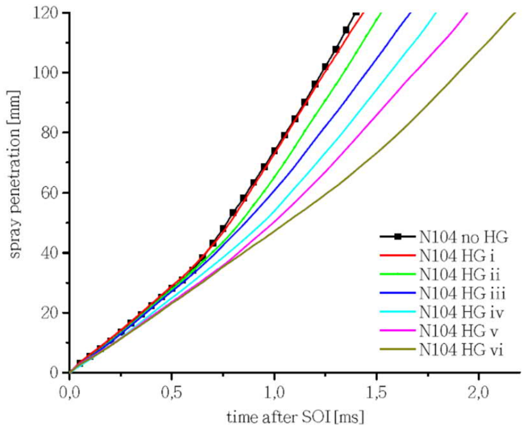

Figure 16: Spray axis of the three different nozzles for various levels of hydro-erosive grinding [19].

Figure 17: Spray penetration curves of the three different nozzles for various levels of hydro-erosive grinding [19].

The three nozzles spray axes behave very differently. The most significant change has the angled nozzle N105 which achieves a total axis angle change of approximately 15°. All the three nozzle types have in common, that the spray axis is not matching the symmetrical axis (0°) of the nozzle bores before applying HG. The eccentric nozzle remains the closest to the symmetrical axis even for significant amounts of HG. The evaluated data depicted in Figure 16 indicate that the spray axis deviations are quite significant and that HG, in general, does not reduce the deviation.

Another important spray morphology parameter is spray penetration. Figure 17 shows the spray penetration for various levels of HG of the nozzle N104. The data is depicted as lines for visibility reasons, however, the data is discrete as indicated with the curve *N104 no HG* and its markers. The x-axis shows the time after the start of injection (SOI). Compared with the in-nozzle pressure data depicted in Figure 13, it becomes clear why the spray penetration speed is reduced with increasing level of HG: the reduced flow resistance and lower fuel pressure due to increasing HG prolong the pressure build-up time in the nozzle main bore and therefore reduce the fluid velocity and penetration speed. The significant pole between 0.5 and 1 ms after SOI originates from the extended pressure build-up time (compare with pressure data in Figure 13) with increasing HG. The spray penetration is slower until the static pressure has built up to its quasi-steady-state in the nozzle main bore.

4 Combustion investigations

4.1 Introduction

To link the in-nozzle flow and spray morphology characteristics of the three different nozzle types to the combustion behavior, the nozzle material was changed to steel in order to withstand the harsh environment. The combustion experiments were performed in the SCC at WinGD. Note that six nozzle setups were investigated: the three nozzles as depicted in Figure 5 and their maximal HG versions from the spray investigation measurements as described in the previous chapter. The metal nozzles were iteratively hydro-erosive ground and characterized using mass flow measurements until the transparent PMMA nozzles and the metal nozzles had identical mass flow properties.

4.2 Experimental setup

The SCC has been operated with a back pressure of 50 bar and gas temperature of approximately 900 K. The fuel injection duration and rail pressure were kept identical as in the previous experimental studies. A total of 20 injections with the same Diesel fuel as in all the previous experiments were acquired per nozzle type. A multi high-speed camera optical setup was chosen and is depicted as a schematic in **Error! Reference source not found.** as a top view with the SCC (b) and cut-off regenerator (g) in the middle.

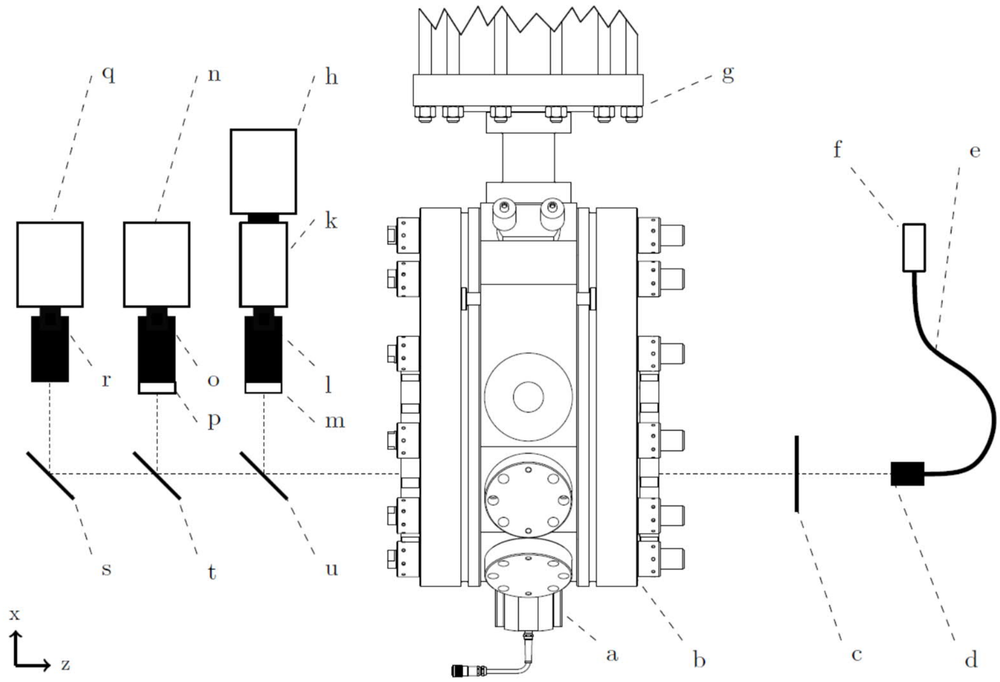

Figure 18: Schematic top view of the spray and combustion chamber (SCC) with the optical setup used. Fuel injector (a), SCC main body (b), diffuser plate (c), collimator (d), light fibre (e), diode laser (f), SCC regenerator (g), high-speed camera 1 (h) with image intensifier (k), UV lens (l) and filter (m), high-speed camera 2 (n) with lens (o) and filter (p), high-speed camera 3 (q) with lens (r), mirror (s), mirror (t) and high-pass filter (u) [4].

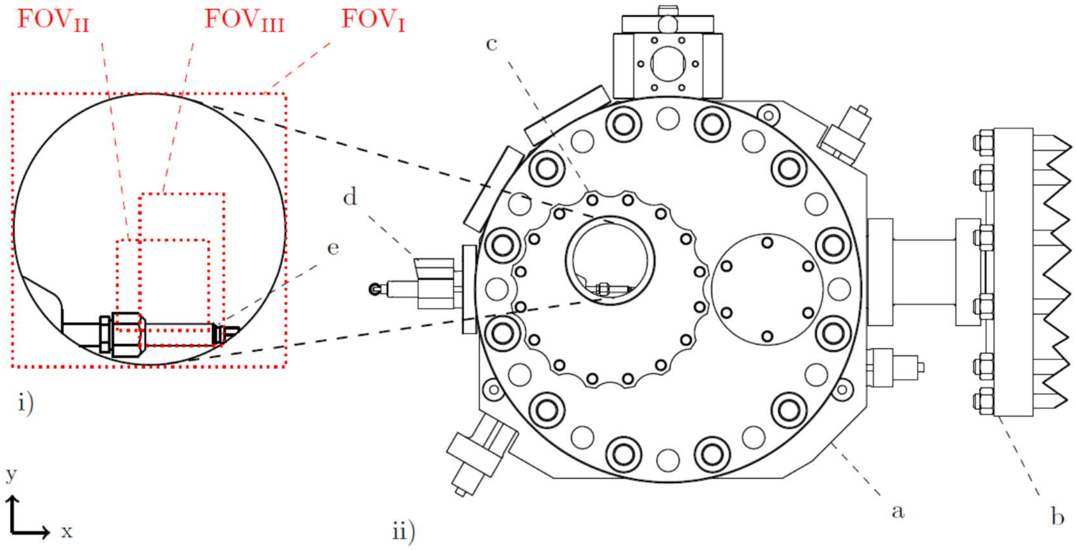

Figure 19: Schematic side view of the spray and combustion chamber (SCC) (ii) indicating the optical access and the enlarged view through the optical windows with the three different field of views (FOV) used (i). SCC main body (a), SCC regenerator (b), side flange with optical access through sapphire windows (c), fuel injector (d), and nozzle (e). The three different fields of view (FOV$_I$, FOV$_{II}$ & FOV$_{III}$) are illustrated using dotted rectangles in the detailed view (i) [4].

The three identical high-speed cameras (h, n, q) were used to measure four different image sets with three different fields of view (FOV). The following four configurations have been run and acquired:

- spray images at 512 x 512 pixel (FOV$_I$) with a frame rate of 20 kHz using Shadowgraphy with a diode laser light source (f)
- flame luminosity images at 512 x 512 pixel (FOV$_I$) with a frame rate of 20 kHz
- spray images at 192 x 192 pixel (FOV$_{II}$) with a frame rate of 100 kHz using Shadowgraphy with a diode laser light source (f)
- OH*-chemiluminescence images at 256 x 448 pixel (FOV$_{III}$) with a frame rate of 40 kHz using a lens-coupled intensifier (k)

The three different FOV are illustrated in Figure 19 (i) together with the side view of the SCC (a). Note the enlarged detail (i) where also the installed metal nozzle is depicted. Although different looking than the TNH from the previous experimental campaigns, the relevant geometrical properties were kept completely identical. The four image sets were used differently to evaluate the combustion behavior of the six different nozzles. The ignition spot locations were evaluated using the OH* signals from the FOV$_{III}$. The spray images using the 100 kHz frame rates (FOV$_{II}$) were used to evaluate the spray morphology before ignition as well as the effective start of injection (SOI). The larger spray images (FOV$_I$) were used for spray and flame morphology evaluations and the flame luminosity images (FOV$_I$) were used to evaluate the flame morphology and flame lift-off length. In addition, the high-speed cameras, the use of an optical light probe (OLP) prototype from Kistler with an ultraviolet bandpass filter for OH* in front of a photomultiplier allowed the acquisition of the start of ignition (SOI) with a very high temporal resolution of 1 MHz. The in-nozzle pressure of the metal nozzles has also been measured for comparison reasons, however, those measurements were performed under ambient conditions to prevent the destruction of the pressure sensor.

4.3 Results

The most important combustion characteristics evaluated from the measurements are shown as averages (µ) with corresponding standard deviations (σ) in Table 1. Note that the values are averaged only over the quasi-steady-state fuel injection period between 6 and 14 ms (compare with in-nozzle pressure curves depicted in Figure 13 and Figure 20). The six metal nozzles used are separated between sharp-edged (*N101*, *N104,* and *N105*) and hydro-erosive ground design (*N101 HG*, *N104 HG,* and *N105 HG*).

Table 1: Measured characteristics for the three sharp-edged and the three hydro-erosive ground nozzles. The data shown are the mean (µ) values together with the standard deviation (σ) [4].

		sharp-edged						hydro-erosive ground					
		N101		**N104**		**N105**		**N101 HG**		**N104 HG**		**N105 HG**	
		µ	SD	µ	SD	µ	SD	µ	SD	µ	SD	µ	SD
in-nozzle pressure	[bar]	378.9	8.2	368.9	9.4	379.0	9.5	360.5	14.3	357.3	14.7	359.4	14.5
injected mass	[g]	0.667	0.013	0.892	0.017	0.874	0.019	1.425	0.032	1.914	0.012	1.411	0.052
flame lift-off length	[mm]	24.8	4.4	31.5	5.0	30.9	4.6	38.4	6.9	29.1	3.5	34.6	5.2
start of ignition	[ms]	0.30	0.01	0.47	0.03	0.39	0.04	1.06	0.06	1.24	0.1	1.05	0.13
spray angle	[deg]	14.5	0.8	16.4	2.1	14.2	0.9	16.3	0.4	23.3	0.8	17.2	1.1
spray axis	[deg]	+ 0.9	0.2	- 0.7	0.5	- 0.9	0.2	+ 0.4	0.3	+ 1.2	0.3	+ 0.6	0.3

The in-nozzle pressure values were measured together with the injected mass using a closed tube to dissipate the energy and a total of 100 injections per nozzle. The total injected Diesel fuel has then been evaluated gravimetrically and calculated to injected mass per injection. Note that those measurements were performed under ambient gas conditions and have a small systematic error as a result.

The measured in-nozzle flow pressure of the six different nozzles is depicted together with the measured injection current of the fuel injector inFigure 20. Note the identical behavior of the pressure curves for the nozzle N104 when compared to the previous measurement campaign as depicted in Figure 13.

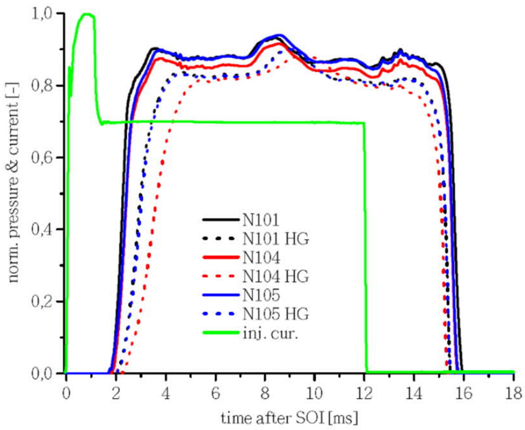

Figure 20: Normalized and averaged injection current and in-nozzle pressure for the various nozzle types measured [4].

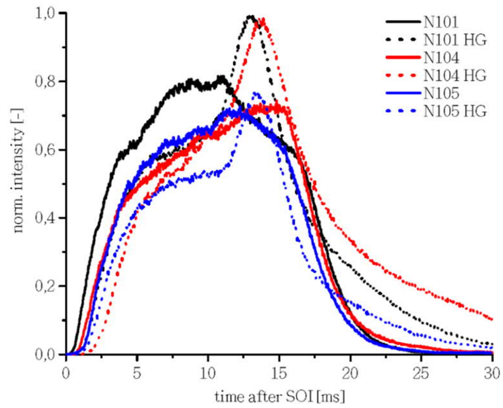

Figure 21: Normalized optical light probe (OLP) signal for the various nozzle types measured [4]. Note that the x-axis represents the start of injection.

The OLP signals used for evaluating the exact start of ignition are plotted in Figure 21. Note that the x-axis represents the start of injection (SOI). When comparing the OLP plot and the averaged data of the start of ignition in Table 1, it becomes clear that there is a significantly earlier ignition for the sharp-edged nozzles with N101 being the earliest and N104 HG the latest. The distinctive peak in the OLP signal after 10 ms for the HG nozzles can be explained with the increased area combusting at the stop of injection since the turbulent diffusion flame reaches back towards the nozzle bore exit. This effect is more prominent with the HG nozzles since significantly more fuel is injected compared with the sharp-edged nozzles (see injected mass in Table 1).

The spray contours have also been averaged and are plotted in Figure 22. Note that the field of view is relatively small since the flame lift-off length is in the area of roughly 30 mm above the nozzle bore exit and the combustion falsifies the spray contour.

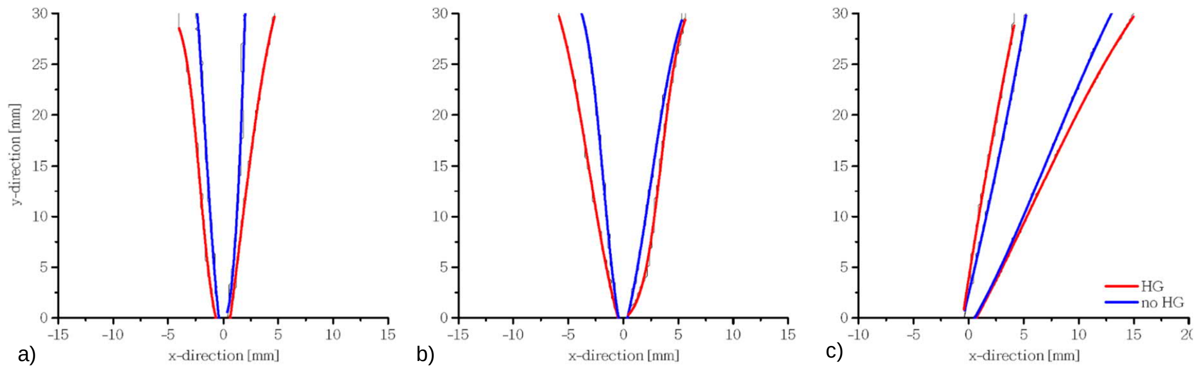

Figure 22: Averaged spray contours of sharp-edged (no HG) and hydro-erosive groud (HG) nozzle types N101 (a), N014 (b), and N105 (c) [4].

The evaluated axis and angles have only limited comparability with the previous experimental campaign since the combustion sprays are under the influence of the gas swirl motion defined by the SCC geometry and reproducing real gas conditions before fuel injection as found at top-dead-center of a typical WinGD engine matching the same bore. However, the differences and especially the spray axis deviations and spray angles are clearly visible from the data provided in Table 1 and Figure 22.

The evaluated ignitions spots are depicted as averaged locations with its standard deviations as error bars and plotted over the averaged spray images closest to the start of ignition. The results are shown in Figure 23 for the sharp-edged nozzles and in Figure 24 for the HG nozzles. Note that the two figures use the same image scale and are therefore directly comparable.

Due to the advanced spray atomization of the sharp-edged nozzles, the start of ignition is two to three times earlier compared with the HG nozzles. This can be seen when comparing the much further developed sprays in Figure 24 with the sprays in Figure 23: the sprays of the HG nozzles penetrate the combustion chamber much deeper before ignition compared to the sharp-edged nozzles. The ignition spot standard deviations tend to become larger with HG as well although the eccentric nozzle *N104 HG* is the exception; it has by far the most stable ignition spot. This may be explained with the strong and stable cavitation swirl motion of the in-nozzle flow. However, the start of ignition has still a significantly higher standard deviation compared with the sharp-edged design of nozzle N104.

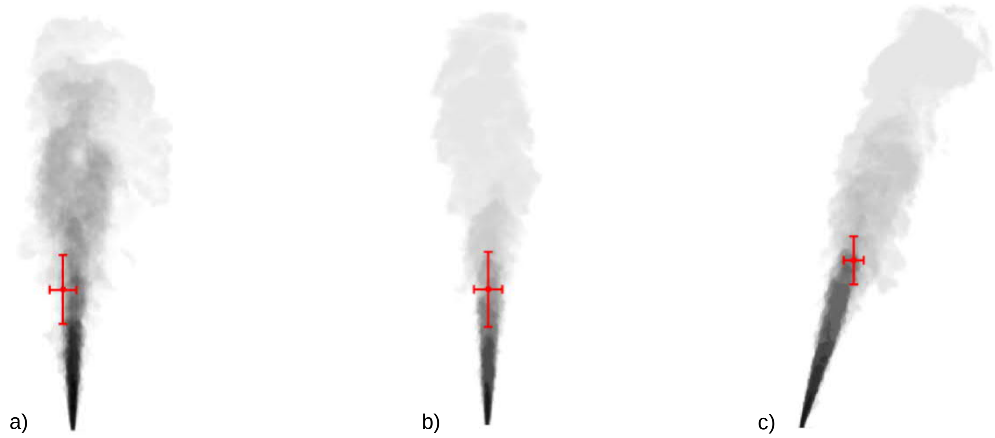

Figure 23: Averaged spray images at the start of ignition (SOI) with mean ignition location and standard deviation for the sharp-edged nozzles N101 (a), N104 (b), and N105 (c) [4].

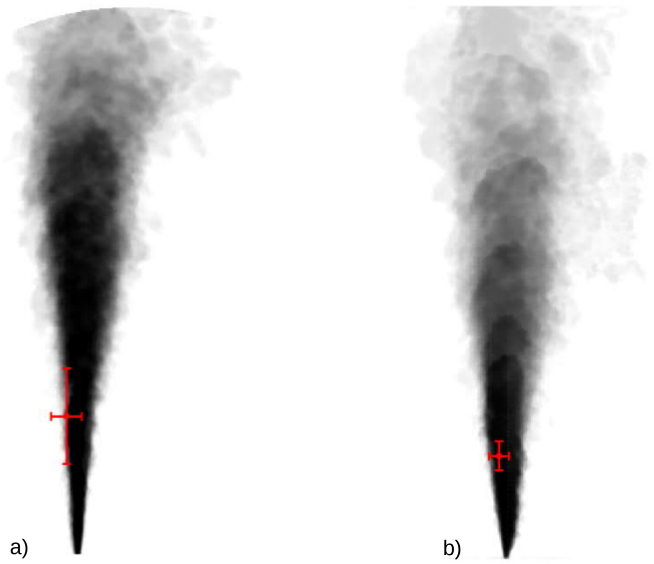

Figure 24: Averaged spray images at the start of ignition (SOI) with mean ignition location and standard deviation for the hydro-erosive ground nozzles N101 HG (a), N104 HG (b), and N105 HG (c) [4].

5 CFD validation

5.1 Introduction

Modeling turbulent cavitating flows is a challenging task because of the complexity of the phenomenon itself and the highly dynamic interaction between phases and non-equilibrium thermodynamic states, however, recent numerical simulations have proven the applicability of CFD in cavitating flow prediction [22] [23] [24] [25]. For the results simulated in this project, the widely applied Volume of Fluid (VOF) method has been chosen together with RANS simulations to solve the transport equation of the volume fraction and to predict the cavitation inside the nozzle bore. The VOF method is suitable to capture small to large scale deformations and interface zones; a Eulerian-Eulerian method, where the liquid and vapor treated in separate phases. The cavity shape is constantly tracked and updated until the local pressure inside the cavity reaches the vapor pressure, therefore giving precise and convergent modeling of the cavity-surrounding liquid interface. The VOF method is able to successfully predict the separation point, recirculation zone and reattachment points. Furthermore, the pressure distribution inside the compressible flow is also correctly captured. The solved transport equation of the vapor fraction predicts the convection of bubble nuclei or micro-bubbles within the liquid caused by cavitation. The method reconstructs the interface location and orientation within each fluid cell.

Validated CFD models are of great use to perform extensive parameter studies which are cheaper and faster than experimental research, even if only valid in a small range of boundary conditions. However, the predictive quality of spray formation, although already on a high level, is still limited [25]. One major problem is the grid size dependence of Eulerian-Lagrangian models; in contrast to the pure Eulerian modeling, a reduction of the grid size does not automatically result in more accuracy [25]. Another problem is the modeling of the atomizing primary breakup together with the cavitational in-nozzle flow; the most popular model nowadays is the *Blob injection method* [25] which assumes that the initial jet breakup and subsequent drop breakup cannot be differentiated in the dense spray region and therefore continuously adds mono-sized *blobs* during injection with a size based on the nozzle bore diameter. As a consequence, another model for further primary breakup is required and careful tuning of the model constants is required for a successful application. The standard cavitation models added to the *blob injection method* are usually one-dimensional models that calculate the effective nozzle area by using empirical correlations; the cavitation effects on breakup outside the nozzle are not included in these standard models [25]. As a consequence, the CFD simulations for this project have been set up in a two-step approach: first, simulate and validate the in-nozzle flow using a Eulerian-Eulerian (VOF) modeling approach using RANS turbulence modeling and calculate the velocity distribution at the nozzle bore exit, and second, use the velocity profile from the in-nozzle flow simulations as a boundary condition for a Eulerian-Eulerian (VOF), one-way coupling approach using LES turbulence modeling for the spray simulations.

5.2 Results

A vertical cross-section cutting the nozzle bore exactly in the middle and visualizing the density distribution inside the nozzle is depicted in Figure 25 i). The density distribution shows not just a separation of flow at the sharp nozzle bore inlet, but also a flow detachment close to the nozzle bore exit, which has a pronounced effect on the spray formation. The local pressure at the nozzle bore inlet drops below the vapor pressure of the fuel at the given temperature level and additionally, the sudden geometrical change invokes immediate cavitation inception. Streamlines colored by velocity magnitude (see Figure 25 ii)) show the path of the fuel inside the nozzle, where the *vena contracta* represented by the compressed streamlines after the fuel enters the nozzle bore from the main bore. A more pronounced separation can be seen on the upper side of the nozzle bore, which is expected since the fuel enters directly from the nozzle main bore inlet direction, therefore suffering a significant redirection caused by the geometrical properties of the nozzle.

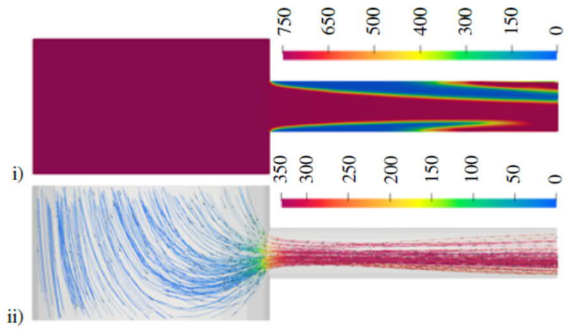

Figure 25: Density distribution [kg/m^3] shown in a vertical section cut in the middle of the nozzle bore (side view) for the nozzle type N101 (i) while streamlines colored by velocity magnitude [m/s] give the flow path inside the nozzle (ii) taken at the end of the simulation [18].

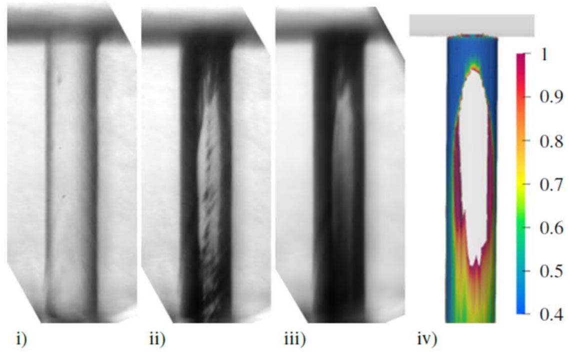

Figure 26: Experimental in-nozzle flow images showing background (i), single-shot (ii), and average during injection (iii) together with the corresponding CFD result (iv) depicting isovolumes of cell fuel vapor pressure fraction in a non-dimensional range for the nozzle N101 [18].

The nozzle design N101 is *supercavitating* as the gaseous phase reaches the nozzle bore exit (see Figure 26). The fuel flow enters the main bore from the left side and hence the cavitation in the nozzle bore on the left side is more distinctive. At the nozzle bore inlet, the flow is fully cavitating around the nozzle bore inlet circumference, however, after approximately one times the diameter of the nozzle bore, the cavitation is limited to the two side walls. Transient cavitation phenomena in the middle of the nozzle bore, as visible in the single-shot image (ii), expand in cavitation volume towards the exit and result in darkening the averaged image (iii) towards the bottom.

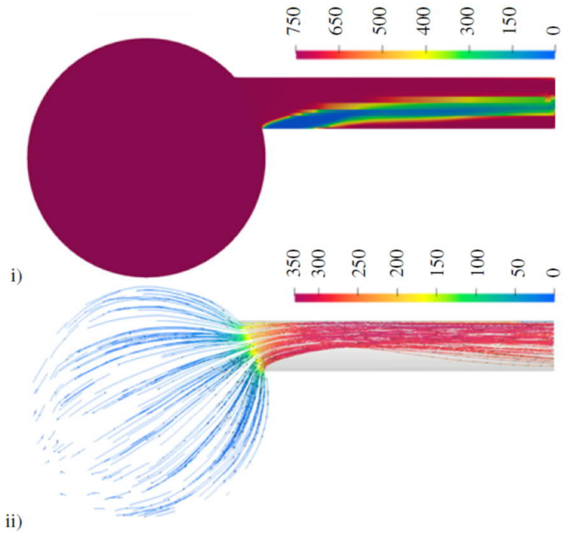

Figure 27: Density distribution [kg/m^3] shown in a vertical section cut in the middle of the nozzle bore (top view) for the nozzle type N104 (i) while streamlines colored by velocity magnitude [m/s] give the flow path inside the nozzle (ii) taken at the end of the simulation [18].

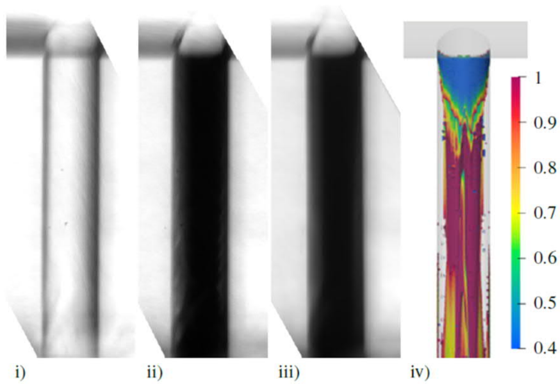

Figure 28: Experimental in-nozzle flow images showing background (i), single-shot (ii), and average during injection (iii) together with the corresponding CFD result (iv) depicting isovolumes of cell fuel vapor pressure fraction in a non-dimensional range for the nozzle N104 [18].

The CFD result predicts a very similar phenomenon as the measurement; chosen isovolumes of cell fuel vapor pressure fraction in a non-dimensional range of 0.4 to 1 visualize the vapor formation along the entire nozzle bore. As in the experimental images, the presence of a coherent vapor layer on the upper and lower walls of the bore extends to the nozzle bore exit and indicate a *supercavitation* cavitation pattern (Figure 26 iv)). The cavitating flow simulation results of the eccentric nozzle type N104 are depicted in Figure 27. The figure describes the flow field in terms of density distribution and velocity field inside the nozzle. The flow enters the nozzle bore through a huge distortion caused by the sharp inlet of the nozzle bore inlet. Flow separation inside the nozzle bore on the nozzle main bore symmetry side occurs and as a result, a huge recirculation zone is created where this region is filled by fuel vapor. The region extends until the nozzle bore exit forming a massive vapor tube inside the nozzle bore and therefore significantly reducing the effective area. The eccentric side of the nozzle bore seems to be undisturbed by the geometry and as a result, the presence of a remarkably high-velocity zone can be found. The highly non-uniform velocity distribution is an obvious outcome of the nozzle bore eccentricity and the geometrically induced cavitation which is suggested by the presented CFD results depicted in Figure 27. Due to the axis of the eccentricity, the cavitation pattern refracts most of the incoming light away, resulting in an almost completely dark nozzle bores (see Figure 28). The single-shot (ii) scarcely reveals non-cavitating zones on the left and right side of the nozzle bore indicating that the *supercavitation* zone is rotated into the optical axis.

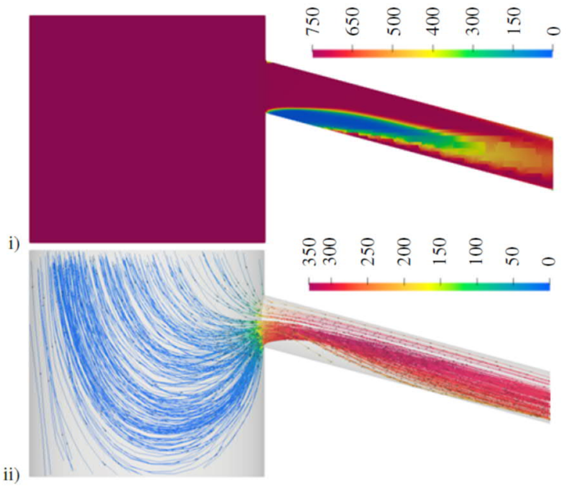

Figure 29: Density distribution [kg/m^3] shown in a vertical section cut in the middle of the nozzle bore (side view) for the nozzle type N105 (i) while streamlines colored by velocity magnitude [m/s] give the flow path inside the nozzle (ii) taken at the end of the simulation [18].

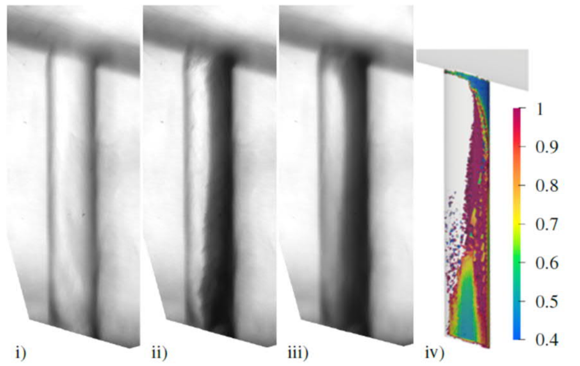

Figure 30: Experimental in-nozzle flow images showing background (i), single-shot (ii), and average during injection (iii) together with the corresponding CFD result (iv) depicting isovolumes of cell fuel vapor pressure fraction in a non-dimensional range for the nozzle N105 [18].

The fuel flow also enters the horizontal main bore from the left side although the cavitation patterns at the nozzle bore inlet indicate strong flow lines from the right side. This is due to the flow pattern in the nozzle main bore that diverts the flow as visible in the streamline CFD result for nozzle N105 in Figure 29 ii). The simulation is in a very good agreement with the experiments (see Figure 28 iv)). The asymmetric vapor formation is well captured, while the locations of the cavitating zones are also corresponding to the results of the optical measurements.

The CFD results of the angled nozzle type N105 are depicted in Figure 29. The figure helps in understanding the flow behavior inside such a nozzle type. The density distribution (Figure 29 i)) shows an extended separation zone on the bottom side of the nozzle bore initiated by the sudden geometrical change at the nozzle bore inlet. Further on, this zone evolves into the fluid domain, compressing the velocity streamlines (see Figure 29 ii)) to the upper side of the nozzle bore creating an area with high velocities. The upper edge of the nozzle bore inlet shows a small depression zone which can be identified as *cavitation inception* at the nozzle bore inlet, although it does not seem to have a significant effect on the flow field. The nozzle N105 shows the most moderate level of cavitation compared to the other two nozzle designs (see Figure 30). The images are rotated so that the nozzle bore walls appear vertical. As a result, the nozzle main bore on the upper side of the images is angled. The fuel enters the main bore from the left side and the nozzle is also *supercavitating*, although only on the right side where the entry between main and nozzle bore remains the sharpest. There are some additional small cavitation patterns at the nozzle bore inlet, but they dissipate immediately leaving all cavitation to one side of the nozzle bore. This can also be realized by examining the results of the numerical simulation (Figure 30 iv)). The small dark area on the left side at the nozzle bore exit, is an optical distortion and not cavitating flow as clearly visible by comparing the background (i) with the single-shot (ii) and averaged (iii) images.

The velocity profiles at the outlet of the nozzle bore have been evaluated from the in-nozzle flow simulations and set as boundary conditions for LES-VOF simulations. Figure 31 shows the evaluated velocity profiles from the validated CFD in-nozzle flow models. The non-homogenous velocity distributions are distinctive and differ significantly with the nozzle geometry changes. The LES spray simulations were limited to a domain length of 10 mm to minimize the total number of cells and therefore reducing computation time. The first spray results are depicted as VOF in Figure 32, where a cross-section (a) and an isosurface (b) illustration are illustrated next to each other for gas and fuel properties as used in the combustion experiments at the SCC.

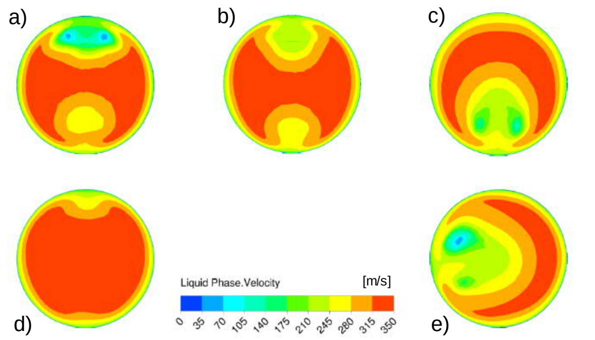

Figure 31: Velocity profiles at the beginning of the spray for different geometrical conditions: nozzle N101 (a), conical angle of 1° (b), N105 (c), inlet radius of 0.5 mm (d) and N104 (e).

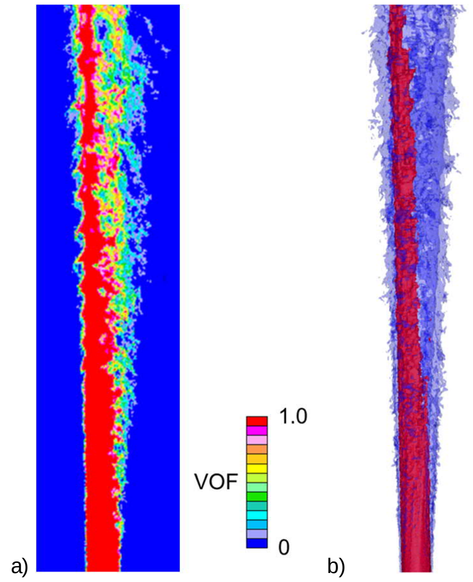

Figure 32: LES-VOF simulation results of eccentric nozzle design N104 showing cross-section (a) and isosurface illustration using red for VOF=0.99 and blue for VOF=0.01 (b).

By comparing the LES-VOF spray isosurface as depicted in Figure 32 b) with the according experimental spray images in Figure 12 a) it becomes clear that the simulation results qualitatively match the experimental data: in both visualizations, one can see the denser region of the spray tending towards the left side while the right side of the spray shows some pronounced atomization and therefore reduced density. However, due to the large computational effort, the validation and evaluation of the spray simulations are still ongoing.

6 Discussion

The in-nozzle flow results qualitatively reveal the strong cavitation patterns, quasi-steady-state and transient, for realistic fuel injection conditions. The developed TNH proved to withstand the high fuel pressures for a relevant number of injections and the technology can be used for further and upcoming research. The transparent nozzles made from PMMA are easy and cost-efficiently machinable and therefore allow fast and cheap investigations of various nozzle geometries. The developed hydro-erosive grinding rig allows to manufacture realistic inlet radii in PMMA and metal nozzles and proves to be a valuable rig for future purposes in the nozzle optimization development at WinGD. Unfortunately, the acquired in-nozzle flow data is limited to qualitative data and the extra effort towards quantitative results like velocity measurements using a PIV method, for example, could not be achieved within the scope of the project.

Ballistic imaging as optical measurement technique to investigate the primary spray breakup revealed strong limitations of the method in connection with large marine two-stroke Diesel injector nozzles at realistic fuel pressures. The nozzle bore diameter used seemed too large and the applicable FOV too small to achieve the desired results. The visualization of a liquid core was not possible with the fuel pressures applied. Even breakup phenomena such as ligament formations could not be detected during the quasi-steady-state injection period. The optical density of the spray was just too high for the optical measurement technique. The limited resolution and quantitative capabilities of BI further reduced the usability of the acquired images for the project purpose.

The spray morphology and combustion measurements performed at the SCC in Winterthur turned out to be the most valuable quantitative data acquired in this project. The data generated and evaluated allowed to link quantitative data with the unfortunately only qualitative results from the in-nozzle flow visualizations. Being able to purchase and to borrow additional optical measurement technique equipment from WinGD’s research partners allowed to test and successfully apply new acquisition setups at the SCC, like applying Shadowgraphy and OH*-chemiluminescence with larger frame rates (100 kHz instead of 20 kHz, and 40 kHz instead of 20 kHz, respectively) and more detailed imagery using a far-field microscope. This new optical setups and evaluation routines established during this project will be the new standard for future optical measurements at the SCC at WinGD. The combustion results showed strong differences with the nozzle geometries investigated and the data generated and evaluated is very helpful to further deepen the understanding of the complex dependency of cavitation in-nozzle flow on spray formation and combustion. However, one big unknown remains with the geometrical differences between PMMA and metallic nozzles; since there is currently no hardware available at WinGD to 3D scan the silicone casts of the nozzles it remains an assumption that the hydro-erosive grinding of the metal and PMMA nozzles generate the identical geometries. Although the mass flow has been gravimetrically matched and the nozzle bore diameters are identical, it is not certain that the abrasive erosion process works the same way and therefore generates the exact same inner geometry for the two completely different materials metal and PMMA.

The CFD models of the in-nozzle flow of the sharp-edged nozzle design could be validated and show good agreement with the experimental results. Due to the lack of a possibility to reproduce the inlet radii of the hydro-erosive ground nozzles into a 3D geometrical model, the CFD model could not yet be extended to the hydro-erosive ground nozzles. However, based on the experience with the sharp-edged nozzle designs it can be assumed that CFD results of similar accuracy can be achieved using the nozzle geometry data with inlet radii. The performed simulations also reveal the importance of the nozzle main bore geometry, especially the closed bottom part where the flow has to recirculate to enter the nozzle bore. This additional informations gained from the three-dimensional, validated in-nozzle flow simulations allow to better understand the individual geometrical influences (angles, diameters, inlet radii, nozzle bore convergence, etc.) and enhances the way the nozzles can be designed.

On the other side, the CFD spray investigations lack behind the expectations from when the project has been set up. The generated results are not yet fully validated and simulations are still ongoing. This is mainly due to the very complex topic of spray formation CFD simulations which is still a very fundamental research topic that uses extensive computational and modeling effort and therefore rather fits academia than industrial research. Additionally, internal changes at WinGD that included a complete software change and personal changes within the CFD group further complicated the scheduled simulation effort. As a result, the focus has moved from detailed simulations of the spray primary breakup towards more industrial research and development worthy spray and combustion simulations of the whole spray. Using the resources available at WinGD (commercial CFD software, limited licenses, limited cluster cores) the CFD simulation efforts are limited to uRANS simulations and hence investigating the primary breakup of an atomizing fuel spray using CFD is very limited. In addition, due to the very simplified model-based approach of the primary breakup simulations and the very limited results gained from the ballistic imaging experimental data, the usability of this task is very questionable. However, spray and combustion simulations on the bigger scale are of great use and unavoidable to further optimize combustion engines and the experimental data generated in this project will help to validate spray models and enhance the predictive spray simulation capabilities of WinGD significantly.

7 Conclusions

The INFLOSCOM project developed and successfully applied a technology to visualize the in-nozzle flow of large marine two-stroke Diesel engine fuel injector nozzles. The technique using transparent nozzles allows to qualitatively visualize the in-nozzle flow conditions under realistic geometrical and fuel pressure conditions. This newly developed technique allows to generate highly accurate quantitative data about cavitation flow in the nozzle bores and hence to produce very valuable CFD models by validating the data. The experimental data gathered in this project showed very strong influences of the nozzle geometries and especially the level of inlet-radii on the spray morphology and combustion. The data provides valuable information about the injected mass, the static and dynamic pressure behavior during fuel injection, and the ignition and combustion properties. It showed phenomenological cavitation behavior which can be used to significantly optimize the fuel injection, spray formation, and combustion. The data acquired and evaluated is unique since the investigated nozzle geometries and applied fuel pressures are in the here used combination not a topic of research in the community which is based on small and medium-sized engines majorly dominated by research on car engines.

Using the knowledge and methods developed in this project will help to further enhance WinGD’s fuel injection process and thus optimize the company’s engines.

The project objectives have mostly been fulfilled and the *out of scope* project targets will be further investigated and evaluated after the end of the project. This will include looking into how cavitation affects the nozzle lifetime, evaluating and validating in-nozzle flow velocities using PIV, and analyzing the in-nozzle pressure data to link its dynamic behavior to the cavitation. The project was able to identify and characterize the major influences of the in-nozzle flow on primary breakup and spray morphology by using transparent nozzles to visualize cavitation together with spray and combustion morphology measurements. A version of the TNH to apply PIV has been designed and built to investigate in-nozzle flow velocities in the near future. The technology developed at Chalmers could successfully be transferred to WinGD to perform measurements under realistic engine conditions at the SCC. The *in-scope* project targets are fulfilled but especially the CFD work on the spray formation and combustion has basically just started delivering valuable results and will last for the next years using data generated in this project and also lead to follow up projects.

8 Outlook

The spray simulations and especially benchmarking the new CFD software used by WinGD (*Converge* instead of *Star-CD*) are ongoing and there will be an enlargement of the WinGD CFD group as well. There will be a follow-up project based on the INFLOSCOM results and other inputs on how to optimize the injector nozzles to achieve higher efficiency with lower emissions.

The results of this project will be presented and distributed internally to disseminate the generated knowledge and evaluate the further steps needed to implement the results into WinGD's daily business with senior experts. The generated validation dataset will be extensively used in the upcoming months to investigate better nozzle designs. Hardware has been ordered to scan silicone molds of the nozzle's interior geometries. This technique will help to generate 3D models of the complex inlet radii between the main bore and nozzle bore and to implement them into the CFD models. Advanced in-nozzle flow CFD simulations, based on the ones performed during this project, can then be set up using these 3D models to evaluate the in-nozzle flow of hydro-erosive ground nozzle geometries and a wide range of parameters can be evaluated to find optimal geometrical conditions for the fuel injection.

The SCC test rig at WinGD will be updated as well to perform more realistic combustion experiments. Using three instead of only one injector and implementing an additional valve between the combustion chamber and the regenerator, to represent the combustion volume at top-dead-center more accurately, will result in acquiring spray and combustion results closer to the experimental engine RTX6 at WinGD. This will help as well to further investigate the in-nozzle and spray behavior of WinGD's fuel injection and help link our generated data better to results acquired on WinGD test engines.

Another upcoming task will be to evaluate the influence of different fuels. While this project only used one fuel for all the experiments, the reality looks quite more complex. There will be a need to further investigate spray morphology and combustion using a very wide spectrum of fuels. The SCC and also the RTX6 test engine at WinGD have both been and are still updated to run with alternative fuels. There will be projects investigating the spray formation and combustion using different nozzle designs and different fuels to compete with upcoming emission regulations.

9 National and international collaboration

On the international level, the project was set up as collaboration together with Chalmers University of Technology, Department of Mechanics and Maritime Sciences, Division of Combustion and Propulsion Systems, in Göteborg, Sweden. The Combustion and Engine Research Center (CERC) affiliated to the Division and direct collaborator is an interdisciplinary engineering research center that is funded by the Swedish Energy Agency, industry, and Chalmers University of Technology itself. The industrial partners are Scania CV AB, AB Volvo, Volvo Car Corporation AB, Delphi Technologies, Winterthur Gas & Diesel Ltd., Neste Oyi, Loge AB, Johnson Matthey, Converge Science GmbH and Wärtsilä.

The division's experience in engine and spray research, especially in the areas of optical measurement techniques and in-nozzle flow investigations has been of great benefit for the project.

10 Dissemination

- Annual CERC seminar in Göteborg on 31st of April 2016 (presentation)
- ECCO-MATE conference in Lund on 07th of May 2016 (poster)
- Annual IEA combustion TCP meeting in Ruka on 27th of May 2016 (presentation)
- CERC meeting in Stockholm on 16th of January 2017 (presentation)
- ILASS Americas conference in Atlanta GA on 17th of May 2017 (presentation & publication)
- Annual CERC seminar in Göteborg on 30th of May 2017 (presentation)
- COMODIA conference in Okayama on 25th of July 2017 (presentation & publication)
- Verbrennungstagung at ETH Zürich on 7th of September 2017 (poster)
- Licentiate thesis defense in Göteborg on 22nd of February 2018 (presentation & publication)
- CAV2018 conference in Baltimore MD on 16th of May 2018 (presentation & publication)
- Annual CERC seminar in Göteborg on 29th of May 2018 (presentation)
- Spray seminar at WinGD on 1st of November 2018 (presentation)
- Swedish Energy Agency Seminar in Göteborg on 1st of April 2019 (presentation)
- ILASS Americas conference in Tempe AZ on 13th of May 2019 (presentation & publication)
- Annual CERC seminar in Göteborg on 29th of May 2019 (presentation)
- Verbrennungstagung at ETH Zürich on 24th of June 2019 (poster)

11 Publications

- R. Balz, A. Schmid, and D. Sedarsky, *In-Nozzle Flow Investigations of Marine Diesel Injectors*, ILASS-Americas 29th Annual Conference on Liquid Atomization and Spray Systems (ILASS), Atlanta, GA, USA, May 2017
- R. Balz, A. Schmid, and D. Sedarsky, *Cavitation Flow Visualization in Marine Diesel Injectors*, The Ninth International Conference on Modeling and Diagnostics for Advanced Engine Systems (COMODIA 2017), Okayama, Japan, July 2017
- R. Balz, *In-Nozzle Flow and Primary Breakup Investigations of Marine Two-Stroke Diesel Engine Injectors*, Thesis for the degree of Licentiate of Engineering, Chalmers University of Technology, 2018
- R. Balz, A. Schmid, and D. Sedarsky, *In-Nozzle Flow Visualization of Marine Diesel Injectors with Different Inlet Radii*, 10th International Cavitation Symposium (CAV2018), Baltimore, MD, USA, May 2018
- R. Balz, and D. Sedarsky, *Temperature Dependent In-Nozzle Flow Investigations of Marine Diesel Injectors*, ILASS-Americas 30th Annual Conference on Liquid Atomization and Spray Systems (ILASS), Tempe, AZ, USA, May 2019
- R. Balz, I.G: Nagy, G. Weisser, and D. Sedarsky, Experimental and numerical investigations of cavitation in marine Diesel injectors, manuscript in preparation.
- R. Balz and D. Sedarsky, Simultaneous in-nozzle flow and spray investigations of large marine two-stroke Diesel fuel injectors, manuscript in preparation.
- R. Balz, G. Bernardasci, B. von Rotz, and D. Sedarsky, Influence of nozzle geometry on spray combustion characteristics related to large two-stroke engine injection systems, manuscript in preparation.
- R. Balz, In-Nozzle Flow, Spray and Combustion Investigations of Marine Two-Stroke Diesel Engine Injectors, Doctoral dissertation, Chalmers University of Technology, manuscript in preparation.

12 References

[1] T. Fansler and S. Parrish, "Spray measurement technology: a review," *Measurement Science and Technology,* no. 26, 2015.

[2] M. Linne, "Imaging in the optically dense regions of a spray: A review of developing techniques," *Progress in Energy and Combustion Science,* vol. 39, 2013.

[3] A. Andriotis, M. Gavaises and C. Arcoumanis, "Vortex flow and cavitation in diesel injector nozzles," *Journal of Fluid Mechanics,* vol. 610, 2008.

[4] R. Balz, G. Bernardasci, B. von Rotz and D. Sedarsky, "Influence of nozzle geometry on spray combustion characteristics related to large two-stroke engine injection systems," *manuscript in preparation.*

[5] A. Schmid, B. von Rotz, R. Schulz, K. Herrmann, G. Weisser and R. Bombach, "Influence of nozzle hole eccentricity on spray morphology," in *LASS - Europe 2013, 25th European Conference on Liquid Atomization and Spray Systems*, Chania, Greece, 2013.

[6] Z. Falgout and M. Linne, "Novel design for transparent high-pressure fuel injector nozzles," *Review of Scientific Instruments,* vol. 87, no. 8, 2016.

[7] D. Martynov, D. Mason, M. Heikal , S. Sazhin and M. Gorokhovski, "Modelling of Cavitation Flow in a Nozzle and Its Effect on Spray Development," *Jets,* 2006.

[8] Y. Sun, Z. Guan and K. Hooman, "Cavitation in Diesel Fuel Injector Nozzles and its Influence on Atomization and Spray," *Chemical Engineering and Technology,* vol. 42, no. 1, 2019.

[9] M. Jeshani, "Optical characterisation of cavitating flows in diesel fuel injection equipment," City University London, Doctoral thesis, 2013.

[10] R. Balz, In-Nozzle Flow, Spray and Combustion Investigations of Marine Two-Stroke Diesel Engine Injectors, Chalmers University of Technology: Doctoral thesis, manuscript in preparation.

[11] R. Balz, A. Schmid and D. Sedarsky, "Cavitation Flow Visualization in Marine Diesel Injectors," in *The Ninth International Conference on Modeling and Diagnostics for Advanced Engine Systesm (COMODIA)*, Okayama, Japan, 2017.

[12] S. Martynov, D. Mason and M. Heikal, "Numerical simulation of cavitation flows based on their hydrodynamic similarity," *International Journal of Engine Research,* vol. 7, no. 3, 2006.

[13] M. Mirshahi, J. Nouri, Y. Yan and M. Gavaises, "Link between in-nozzle cavitation and jet spray in a gasoline multi-hole injector," in *ILASS – Europe, 25th European Conference on Liquid Atomization and Spray Systems*, Chania, Greece, 2013.

[14] L. Lešnik, B. Kegl, G. Bombek, M. Hočevar and I. Biluš, "The influence of in-nozzle cavitation on flow characteristics and spray break-up," *Fuel,* vol. 222, no. 4, 2018.

[15] F. Payri, V. Bermúdez, R. Payri and F. Salvador, "The influence of cavitation on the internal flow and the spray characteristics in diesel injection nozzles," *Fuel,* vol. 83, no. 4-5, 2004.

[16] M. Shervani-Tabar, S. Parsa and M. Ghorbani, "Numerical study on the effect of the cavitation phenomenon on the characteristics of fuel spray," *Mathematical and Computer Modelling,* vol. 56, no. 5-6, 2012.

[17] R. Balz, A. Schmid and D. Sedarsky, "In-Nozzle Flow Visualization of Marine Diesel Injectors with Different Inlet Radii," in *10th International Cavitation Symposium (CAV1028)*, Baltimore, MD, USA, 2018.

[18] R. Balz, I. Nagy, G. Weisser and D. Sedarsky, "Experimental and numerical investigations of cavitation in marine Diesel injectors," *manuscript in preparation.*

[19] R. Balz and D. Sedarsky, “Simultaneous in-nozzle flow and spray investigations of large marine two-stroke Diesel fuel injectors,” *manuscript in preparation.*

[20] H. Purwar, S. Idlahcen, C. Rozé, D. Sedarsky and J. Blaisot, “Collinear, two-color optical Kerr effect shutter for ultrafast time-resolved imaging,” *Optics Express,* vol. 22, no. 13, 2014.

[21] D. Sedarsky, E. Berrocal and M. Linne, “Quantitative image contrast enhancement in time-gated transillumination of scattering media,” *Optical Express,* vol. 19, no. 3, 2011.

[22] C. Arcoumanis, M. Gavaises and J. Nouri, “The role of cavitation in automotive fuel injection systems,” in *Proceedings of the 8th International Symposium on Internal Combustion Diagnostics*, Baden-Baden, Germany, 2008.

[23] D. Schmidt, “The internal flow of diesel fuel injector nozzles: A review,” *International Journal of Engine Research,* vol. 2, no. 1, 2001.

[24] J. Hult, P. Simmank, S. Matlok, S. Mayer, Z. Falgout and M. Linne, “Interior flow and near-nozzle spray development in a marine-engine diesel fuel injector,” *Experiments in Fluids,* vol. 57, no. 4, 2016.

[25] C. Baumgartner, Mixture Formation in Internal Combustion Engines, Springer-Verlag, 2006.